3

Urban climate

Processes, trends, and projections

Coordinating Lead Authors:

Reginald Blake (New York City, Kingston), Alice Grimm (Curitiba), Toshiaki Ichinose (Tokyo), Radley Horton (New York City)

Lead Authors:

Stuart Gaffin (New York City), Shu Jiong (Shanghai), Daniel Bader (New York City), L. DeWayne Cecil (Idaho Falls)

This chapter should be cited as:

Blake, R., A. Grimm, T. Ichinose, R. Horton, S. Gaffin, S. Jiong, D. Bader, L. D. Cecil, 2011: Urban climate: Processes, trends, and projections. *Climate Change and Cities: First Assessment Report of the Urban Climate Change Research Network*, C. Rosenzweig, W. D. Solecki, S. A. Hammer, S. Mehrotra, Eds., Cambridge University Press, Cambridge, UK, 43–81.

3.1 Introduction

Cities play a multidimensional role in the climate change story. Urban climate effects, in particular the urban heat island effect, comprise some of the oldest observations in climatology, dating from the early nineteenth century work of meteorologist Luke Howard (Howard, 1820). This substantially predates the earliest scientific thought about human fossil fuel combustion and global warming by chemist Svante Arrhenius (Arrhenius, 1896). As areas of high population density and economic activity, cities may be responsible for upwards of 40 percent of total worldwide greenhouse gas emissions (Satterthwaite, 2008), although various sources have claimed percentages as high as 80 percent (reviewed in Satterthwaite, 2008). Figure 3.1 shows a remotely sensed map of nocturnal lighting from urban areas that is visible from space and vividly illustrates one prodigious source of energy use in cities. Megacities, often located on the coasts and often containing vulnerable populations, are also highly susceptible to climate change impacts, in particular sea level rise. At the same time, as centers of economic growth, information, and technological innovation, cities will play a positive role in both climate change adaptation and mitigation strategies.

Urban population recently surpassed non-urban population worldwide and is projected to grow from 50 percent currently to 70 percent by 2050 (UNFPA, 2007). The urban population growth rate will be even more rapid in developing countries. In terms of absolute numbers, urban population will grow from ~3.33 billion today to ~6.4 billion in 2050, about a 90 percent increase. These numbers underscore the fact that urban climate is becoming the dominant environment for most of humanity.

This chapter presents information on four interrelated components of urban climate: (i) the urban heat island effect and air pollution, (ii) the current climate and historical climate trends, (iii) the role of natural climate variability, and (iv) climate change projections due to worldwide greenhouse gas increases. Figure 3.2 provides a schematic of key interactions within the urban climate system.

Teasing out the relative influences of these components on urban climate is challenging. Natural variability can occur at multidecadal timescales, comparable to the timescales used for historical analysis and to long-term greenhouse gas forcing. Another challenge is that different climate factors may not be independent. For example, climate change may influence the amplitude and periodicity of natural variability, such as the intensity and frequency of the El Niño–Southern Oscillation (ENSO).

To survey these issues, twelve cities are selected as examples. The twelve focus cities in this chapter – Athens (Greece), Dakar (Senegal), Delhi (India), Harare (Zimbabwe), Kingston (Jamaica), London (UK), Melbourne (Australia), New York City (USA), São Paulo (Brazil), Shanghai (China), Tokyo (Japan), and Toronto (Canada) (Figure 3.3) – share a range of characteristics but also differ in key respects. They are all large, dynamic, and vibrant

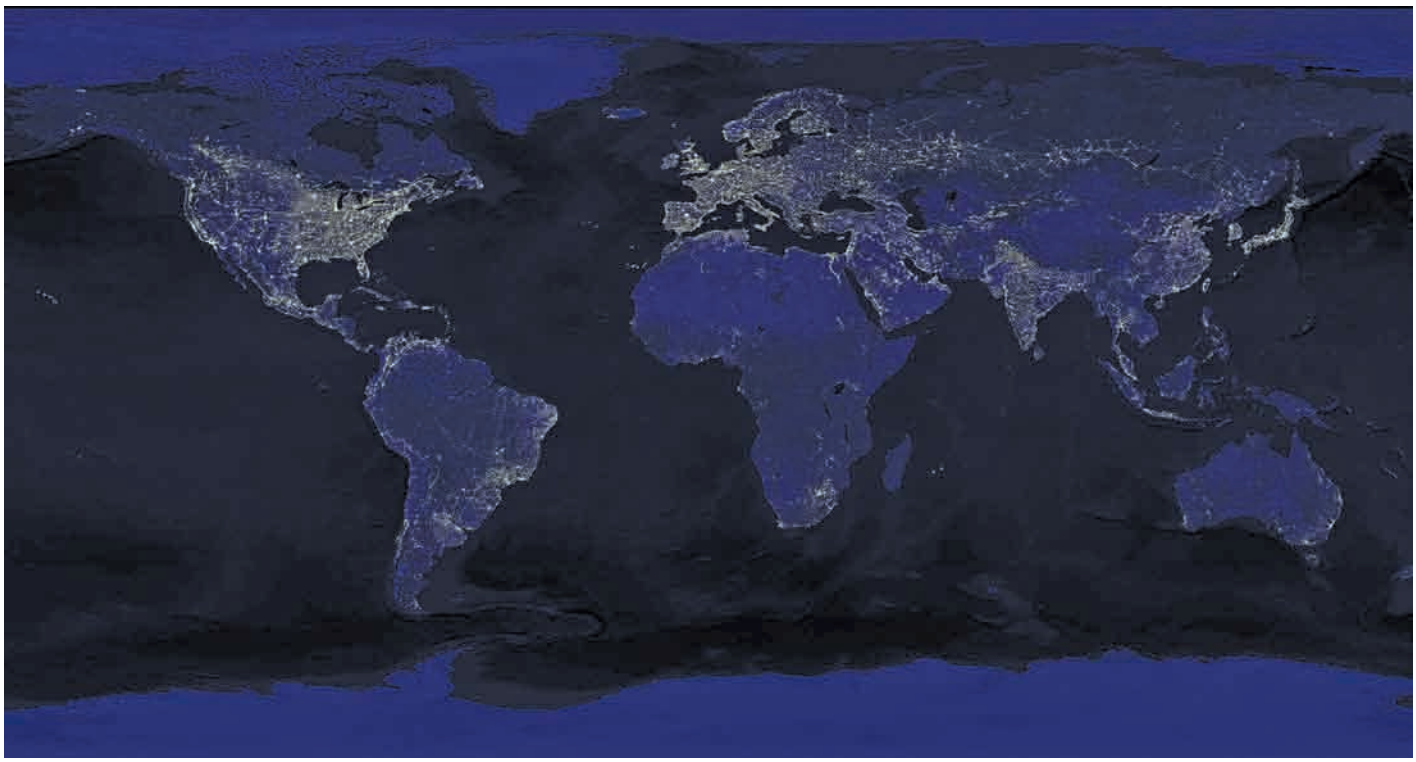

Figure 3.1: *View of Earth at night: Areas of light show densely populated, urban areas.*

Source: NASA

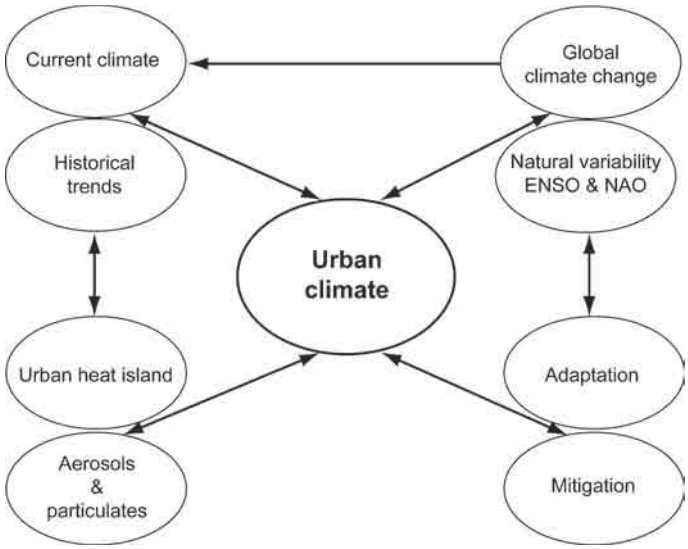

Figure 3.2: *Conceptual framework of this chapter showing major components impacting urban climate.*

urban areas, and act as hubs of social and economic activity. They also feature long-term twentieth-century climate records that allow trend detection, projections, and impact analysis. All the cities selected are likely to experience significant climate change this century, and several illustrate the influence of climate variability systems such as ENSO. Some of the city examples demonstrate unique vulnerabilities to extreme climate events.

With regard to differences, the selection includes a range for geography and economic development levels. The various geographic locations allow examination of climate change impacts in multiple climate zones. Covering multiple climate zones also allows for the examination of the influence of the major natural climate variability systems such as ENSO.

A range of economic development examples is important for vulnerability studies. Adaptation planning for climate change tends to be more difficult in cities with limited resources; typically but not always the case in developing countries. Our focus cities include examples from both the developed and developing world, with some having already taken steps to prepare for climate change and others that have yet to start. Table 3.1 gives some summary statistics on socio-economic and geographic data, and mean climate for the focus cities.

3.1.1 Effects of cities on temperature: urban heat islands

Urban areas are among the most profoundly altered landscapes away from natural ecosystems and processes. Figure 3.4 illustrates a recent reconstruction of the verdant "Mannahatta" island circa 1609 as compared to the current landscape 400 years later (Sanderson and Boyer, 2009). Pondering this visually arresting reconstruction, it is not surprising that cities have altered microclimates with, among other effects, significantly elevated surface and air temperatures.

The elevation in temperatures is most generally explained in terms of the basic surface energy balance processes of shortwave and longwave radiation exchange, latent, sensible, and conductive heat flows (Oke, 1987). With respect to shortwave, or solar, radiation, surface albedo refers to the reflectivity of a surface to visible light and is measured from 0 to 100 percent reflectivity. The regional albedo of cities is significantly lower than natural surfaces due to the preponderance of dark asphalt roadways, rooftops, and urban canyon light trapping. These urban features have typical albedo values below 15 percent (Table 2-4 in Rosenzweig *et al.*, 2006). This leads to efficient shortwave radiation absorption. The urban skyline, with deep urban canyons, results in a greatly reduced skyview at street level and this impedes longwave radiative cooling processes. This urban vertical geometry further impacts winds, generally reducing ventilation and sensible heat cooling. The replacement of natural soil and vegetation with impervious surfaces leads to greatly reduced evapotranspiration and latent heat cooling. The dense

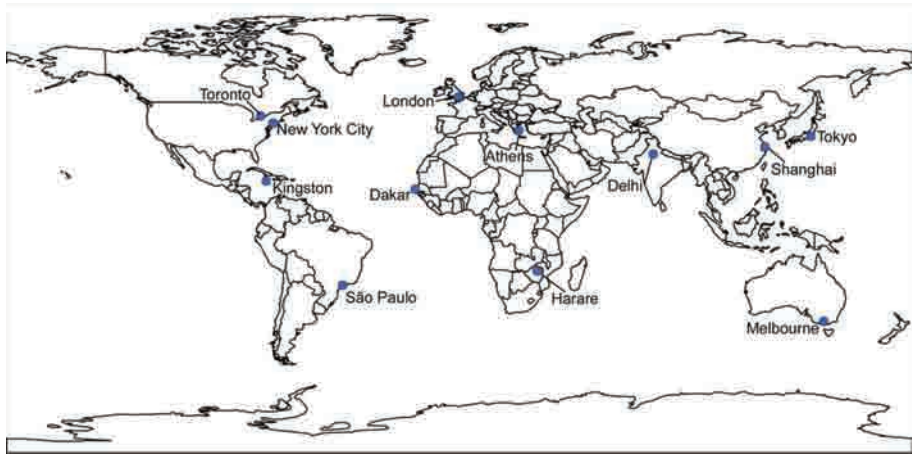

Figure 3.3: *Map of cities highlighted in this chapter. The cities were selected based on socio-economic factors and the availability of long-term climate data.*

Table 3.1: *City statistics and mean temperature and precipitation for 1971–2000.*[*]

City	Latitude	Longitude	Population	Mean annual temperature	Annual precipitation
Athens	37.9 N	23.7 E	789,166 (2001)	17.8 °C	381 mm
Dakar	14.7 N	17.5 W	1,075,582 (2007)	24.0 °C	357 mm
Delhi	28.6 N	77.2 E	9,879,172 (2001)	25.1 °C	781 mm
Harare	17.8 S	31.0 E	1,435,784 (2002)	18.1 °C	830 mm
Kingston	17.9 N	76.8 W	579,137 (2001)	27.5 °C	691 mm
London	51.3 N	0.4 W	7,556,900 (2007)	9.7 °C	643 mm
Melbourne	37.8 S	145.0 E	3,806,092 (2007)	15.7 °C	652 mm
New York City	40.8 N	74.0 W	8,274,527 (2007)	12.8 °C	1181 mm
São Paulo	23.5 S	46.4 W	11,016,703 (2005)	19.5 °C	1566 mm
Shanghai	31.5 N	121.4 E	14,348,535 (2000)	16.4 °C	1155 mm
Tokyo	35.7 N	139.8 E	8,489,653 (2005)	16.2 °C	1464 mm
Toronto	43.7 N	79.0 W	2,503,281 (2006)	7.5 °C	793 mm

[*]Population data for all cities are from the United Nations Statistics Division Demographic Yearbook, United Kingdom National Statistics Office, and Census of Canada. Annual temperature and precipitation statistics are computed for all cities using data from the National Climatic Data Center Global Historical Climatology Network (NCDC GHCNv2), UK Met Office and Hadley Centre, Australian Bureau of Meteorology, and Environment Canada.

Figure 3.4: *Manhattan-Mannahatta: on right is a reconstruction of Manhattan Island circa 1609 (called "Mannahatta" by the Lenape native Americans), as compared to today, based on historical landscape ecology and map data.*

Sources: Markley Boyer / The Mannahatta Project / Wildlife Conservation Society and the aerial view of modern Manhattan, Amiaga Photographers

impervious surfaces with high heat capacity create significant changes in heat storage and release times as compared to natural soil and vegetated surfaces.

There are additional atmospheric and heat source processes in cities that interact with these energy balances. Aerosols tend to reduce the amount of incoming solar radiation reaching the surface (a net cooling effect), while elevated ambient urban carbon dioxide levels may further reduce net radiative cooling.

The high density of population and economic activity in urban areas leads to intense anthropogenic heat releases within small spatial scales. These include building heating and cooling systems, mass transportation systems and vehicular traffic, and commercial and residential energy use. Anthropogenic heat emission has been well documented and researched in developed countries as a major factor causing the heat island phenomenon (Ohashi *et al.*, 2007). As economic development, urbanization, and population growth continue in the developing countries, anthropogenic heat has increased there as well (Ichinose and Bai, 2000). Growth in urbanization increases energy demand in general and electricity demand in particular.

In analogy with the well-established urban heat island, it is tempting to define additional atmospheric urban "islands" such as rainfall islands, and relative humidity islands, which refer to potential urban alterations of precipitation and reductions in urban soil moisture availability due to impervious surfaces. In some cities, there may be good evidence for their existence and effects, such as in Shanghai (Section 3.1.3.1). In general though, the case for additional urban atmospheric islands, such as rainfall islands, is not as straightforward as the heat island and needs further research and characterization.

There can be little question, however, about the broad array of quality-of-life issues that are generally negatively impacted by excess urban heat. These include extreme peak energy demands, heat wave stress and mortality risk, air quality deterioration, seasonal ecological impacts including thermal shocks to waterways following rain events and impacts on urban precipitation.

3.1.2 Effects of cities on local precipitation

There is a longstanding interest in the question of urban impacts on precipitation both locally and regionally. Although there is evidence that urbanization and precipitation are positively correlated, a consensus on the relationship has not yet been reached. Early studies by Horton (1921) and Kratzer (1937, 1956) provided indications that urban centers do play a role in strengthening rainfall activity. Studies by Landsberg (1956), Stout (1962), and Changnon (1968) discussed the extent to which urbanization may induce and strengthen precipitation. The strongest argument used in those studies to substantiate the role of urban centers on rainfall was the enhancement of downwind rainfall. Landsberg (1970) and Huff and Changnon (1972a,b) used observed data to support this hypothesis. Balling and Brazel (1987), Bornstein and LeRoy (1990), Jauregui and Romales (1996), Selover (1997), Changnon and Westcott (2002), and Shepherd *et al.* (2002) have shown evidence that corroborates the earlier findings of enhanced precipitation due to urbanization. However, the hypothesis has been disputed, and even challenged, by other data studies that show no local effect on precipitation (Tayanc and Toros, 1997) or even deficits in precipitation that accompany urbanization (Kaufmann *et al.*, 2007).

Recent studies by Burian and Shepherd (2005) and Shepherd (2006) point specifically to increases in downwind rainfall due to urbanization. Although topological effects may be partially responsible for this finding in the Shepherd (2006) case, Chen *et al*. (2007) supports the Shepherd (2006) study. Shepherd *et al*. (2002) and Simpson (2006) have defined an "urban rainfall effect," which is defined as the impact of urban centers on enhancing downwind and peripheral rainfall. However, there is again no consensus for a unifying theory for the urban rainfall effect. Various explanations of why urbanization positively impacts convection have evolved over the years (Shepherd, 2005). The arguments include sensible heat flux enhancement, urban heat island-induced convection, the availability of more cloud condensation nuclei in urban areas, urban canopy alteration or disruption of precipitation systems, and increased surface roughness convergence.

3.1.3 Climate change impacts on the urban heat island processes

Climate change may well modify the urban heat island and rainfall effects, but the quantitative extents are unknown at this time. This is a ripe area for potential future climate research. For example, warmer winter temperatures may decrease energy combustion for heating, but also increase summertime air conditioning needs, thus affecting these anthropogenic heat sources. Higher temperatures in summer are likely to lead to higher levels of pollutants such as ozone. Changes in temperature, precipitation and ambient levels of carbon dioxide will all impact local vegetation and ecosystems with effects on urban parks and vegetation restoration, which is an important adaptation strategy. Climate-induced changes in winds could also impact urban climate. It should also be noted that urbanization often increases the impact of a given climate hazard. For example, a precipitation event is more likely to produce flooding when natural vegetation is replaced with concrete, and temperatures above a certain level will cause greater mortality when air pollution levels are high.

3.1.3.1 Shanghai: many urban environmental islands

Due to its land use patterns (Figure 3.5) and high densities of population and buildings, Shanghai experiences perhaps five interrelated microclimatic impacts, which we frame as metaphorical "islands" in analogy with the heat island: the heat island, dry island, moisture island, air pollution island, and rain island.

The Shanghai heat island appears from afternoon to midnight under certain weather patterns. According to ground observation records from the past 40 years, there is an apparent mean annual temperature difference of 0.7 °C between downtown and the suburban areas (16.1 °C and 15.4 °C, respectively). The corresponding mean annual extreme maximum temperatures are 38.8 °C and 37.3 °C, respectively. This urban warmth tends to appear from afternoon to midnight in mid autumn and in early winter, summer, and spring under clear conditions with low winds (Figure 3.5).

The second and third Shanghai islands can be referred to as the dry and moisture island effects. The elevated inner city temperatures and greater soil moisture availability in rural areas should result in lower urban relative humidity. Annual average data from Shanghai confirm this effect (Figure 3.5). However, the daily cycle of urban–rural humidity can be more complex due to differences in dewfall, atmospheric stability, and freezing, which can dry out rural air overnight and lead to greater urban humidity at night (Oke, 1987). This can lead to a cycle of relative dry and moisture islands that alternate during the day and night.

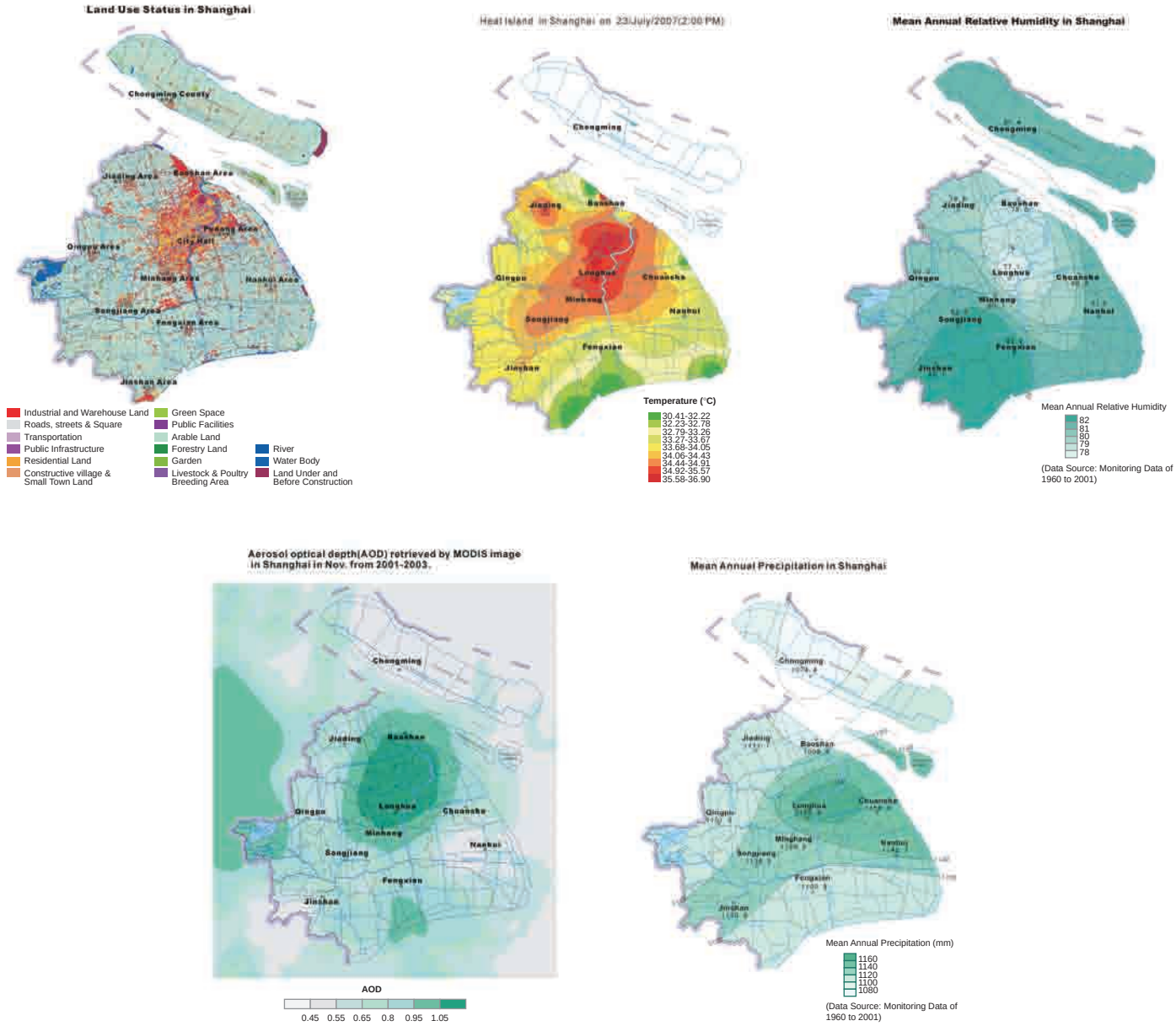

Figure 3.5: *Shanghai urban islands effects. From top left to bottom right are Shanghai's land use pattern, temperature, relative humidity, optical depth, and precipitation. For all the climate variables, a distinct pattern emerges in the area of greatest development.*

Source: Jiong (2004).

These differences in relative humidity may have implications for human comfort indices during heat waves and cold periods.

The fourth island is an air pollution island, since urban air quality is poorer than that of suburban and rural areas. The inversion layer over the urban heat island holds back the diffusion of atmospheric pollutants, increasing pollution levels locally. This in turn leads to acid rain. In 2003, the average pH value of precipitation in Shanghai was 5.21, with a percentage of acid rain of 16.7 percent. In the downtown area, where industry, commerce, traffic, and residents interact closely, air pollution is severe, as shown in Figure 3.5.

The fifth Shanghai urban island is termed the urban rainfall effect. According to ground observation records in the flooding season (May–September) and non-flooding season (October–April in the following year) over the period 1960–2002, the central city experiences greater precipitation than the outlying regions (urban rainfall effect), with an average precipitation that is 5–9 percent higher than in the surrounding regions. There are a number of hypothetical scenarios that may produce an urban rainfall effect: (1) the urban heat island effect may contribute to the rising of local air currents, which help to develop convective precipitation; (2) reduced urban windspeeds may slow the movement of storm systems over urban areas and could lengthen the duration of rain events; (3) aerosol pollutants may provide potential rainfall "nucleation sites" in low-forming clouds over the city. Thus, the urban heat island, the urban wind regime, and the urban pollutant island may all be partially responsible for the higher precipitation amount in the central city and the leeward area (Figure 3.5).

3.2 Natural variability of the climate system

Cities are vulnerable to modes of natural climate variability (that is, not caused by climate change), or preferred oscillations in atmospheric circulation. These preferred oscillations tend to recur at seasonal to multi-year timescales, have somewhat predictable impacts on temperature and precipitation in specific regions, and impact large portions of the planet.

Modes of climate variability centered in one location are able to impact temperature and precipitation in distant regions through a process called teleconnections, whereby wave motions transport energy outward from climate variability source regions along preferred paths in the atmosphere (Hurrel *et al*., 2003). Natural climate variability can cause significant impacts, for example by influencing the frequency and intensity of extremes of temperature and precipitation. It is, therefore, important for stakeholders to recognize these risks, which may be overlooked when assessing climate hazards associated with long-term global change.

Modes of natural climate variability have some level of forecast predictability, which can help cities prepare for climate extremes associated with the modes. However, many cities, especially in the developing world, lack capacity to make forecasts on their own. It must also be kept in mind that these modes of variability are only responsible for a portion of the temperature and precipitation variability experienced by cities. It is therefore not uncommon for cities to experience climate anomalies of opposite sign to what the particular phase of the mode would suggest. For example, in Zimbabwe during the El Niño year of 1997–1998, drought conditions were predicted, and policy decisions were made based on the expectation of drought and reduced maize yields. However, rainfall ended up being above normal, which reduced perceived credibility of climate forecasts (Dilley, 2000). Conveying subtleties such as probability, uncertainty, and risk management to stakeholders around the globe can be a major challenge.

One lesson is that intra-regional rainfall patterns in these El Niño (and other modes) impacted areas can be very complex (Ropelewski, 1999). Another is that, while climate models of projected impacts are improving, achieving accurate seasonal climate predictions months in advance is still a research goal. In addition, with global climate change, patterns of natural climate variability themselves may change (in terms of strength, frequency, and duration of the modes). Even if the modes remain the same, climate change may alter the teleconnection patterns that drive regional climate impacts.

We highlight two specific modes that have large impacts on temperature and precipitation in many cities around the world: the El Niño–Southern Oscillation and the North Atlantic Oscillation. Additional modes are briefly described, followed by a discussion of interactions between climate variability and climate change.

3.2.1 El Niño–Southern Oscillation

Among climate oscillations, the coupled atmosphere–ocean phenomenon, known as the El Niño–Southern Oscillation (ENSO), impacts the most cities worldwide. The oceanic manifestations of this mode, known as El Niño episodes, are mainly characterized by the warming of the tropical central and eastern Pacific. La Niña tends to exhibit the opposite cooling effects. The main atmospheric manifestation, known as the Southern Oscillation, is a seesaw of the global-scale tropical and subtropical surface pressure pattern, which also involves changes in the winds, tropical circulation patterns, and precipitation (Trenberth and Caron, 2000).

ENSO is measured by several indices, including the surface pressure difference between Darwin and Tahiti (Southern Oscillation Index, SOI) and the sea surface temperatures in some selected regions in the central and eastern equatorial Pacific (Figure 3.6). El Niño episodes occur about every three to seven years, but their frequency and intensity vary on inter-decadal timescales.

There are tropical–extra-tropical teleconnections (Figure 3.7) caused by energy transfer from the tropics, which also cause

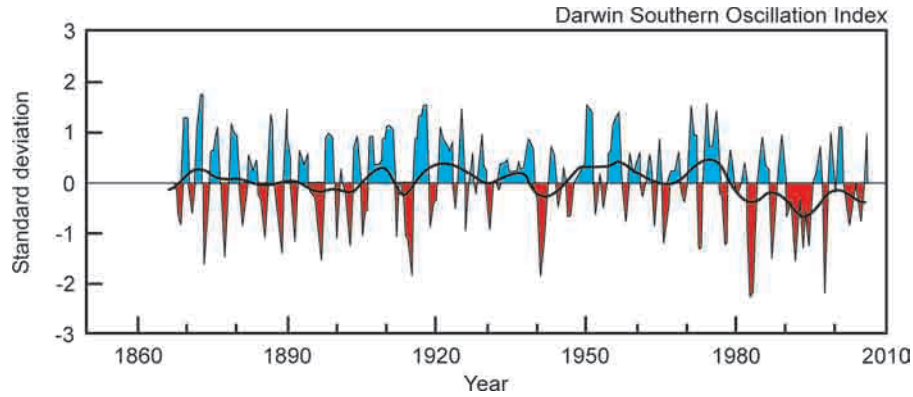

Figure 3.6: *Southern Oscillation Index. The SOI is one measure of the El Niño–Southern Oscillation, a pattern of natural climate variability. Red indicates El Niño episodes, and blue La Niña episodes.*

Source: Trenberth (1989), with data from UCAR/NCAR.

circulation, precipitation, and temperature variations in subtropical and higher latitudes, such as the Pacific–North American (PNA) and Pacific–South American (PSA) patterns. These teleconnections are associated with precipitation anomalies (departures from long-term averages) in cities in South and Southeast Asia, Australia, southern Africa, the southern United States, and tropical and subtropical South America.

The impacts of ENSO vary by season in different regions of the world, and therefore in different cities. For example, in southeastern South America, impacts are strongest during the austral spring (Grimm *et al.*, 2000). Opposite effects may occur in different periods of an ENSO episode, and thus annual anomalies can be weak even if strong anomalies happen during particular months or seasons (Grimm, 2003, 2004). For example, in Jakarta, Indonesia, reduced precipitation in the fall of El Niño years is often partially offset by enhanced precipitation the following spring (Horton, 2007).

Box 3.1 describes the impacts of ENSO in Rio de Janeiro.

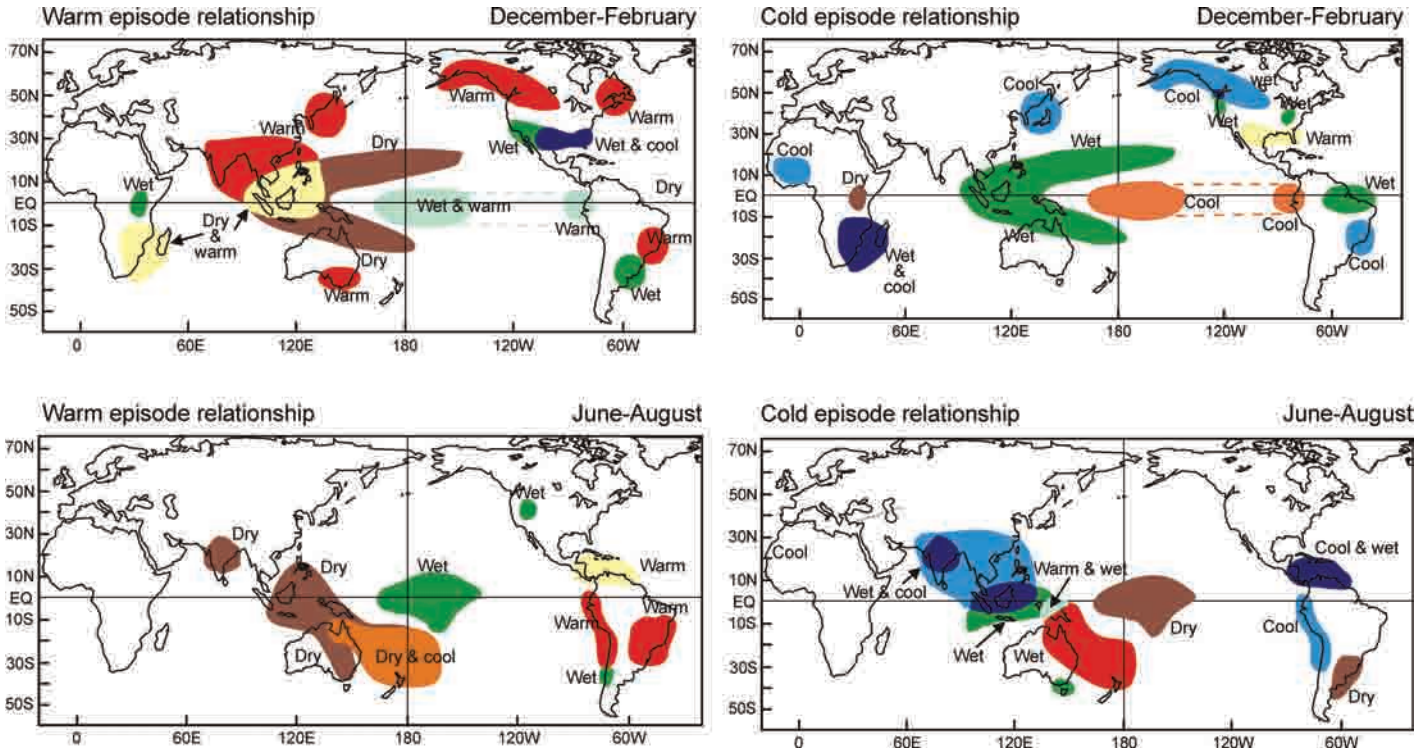

Figure 3.7: *ENSO Teleconnections. Teleconnections for both warm (El Niño) and cold (La Niña) episodes are shown. The variation of the teleconnections by season for each episode is also included.*

Source: NOAA NCEP Climate Prediction Center

[ADAPTATION] Box 3.1 Climate-proofing Rio de Janeiro, Brazil[i]

Alex de Sherbinin

CIESIN, Earth Institute at Columbia University

Daniel J. Hogan

State University of Campinas, Brazil

As flooding and landslides in April 2010 and January 2011 have demonstrated, Rio de Janeiro and the surrounding region continue to be at high risk of climate impacts. Approximately 200 deaths were attributed to the April 2010 floods and landslides, and several thousand people were made homeless, while 450 died in mudslides in the state of Rio de Janeiro in early 2011.[ii] Efforts will need to be made to "climate proof" the metropolitan region, increasing its resilience to floods induced by climate change and variability.

The city and metropolitan region of Rio de Janeiro have populations of 5 million and 11 million, respectively. Guanabara Bay, where Rio is situated, faces almost due south. Rio's dramatic topography has made it prone to landslides and flooding in low-lying areas (Box Figure 1). With the Atlantic rainforest having been stripped away from many hillsides, the thin soils have become prone to landslides, and the granite and gneiss bedrock has been left exposed to weathering, making it more prone to decomposition and erosion.

The coastline in this area was characterized by lagoons, estuaries, and low-lying coastal marshes, many of which have been filled in. The flat topography of low-lying areas, combined with a lack of drainage, has continued to result in flooding during the summer rainy season (January–March). The few remaining lagoons, mangroves, and marshes have been affected by land fill and sedimentation, reducing their absorptive capacity during extreme rainfall events. Low-lying areas around Lagoa de Tijuca and Lagoa de Jacarepaguá will largely be submerged with sea level rise of 0.5–1m.[iii]

The city receives higher than normal precipitation during the summer months of some El Niño events, but the connection with ENSO is not consistent. In the summer of 1998, in the end of an El Niño episode, the city was affected by severe floods as a result of two intense periods of rainfall in early February that produced a total of 480 mm of rain, which constitutes one-third the annual average rainfall of 1,200–1,500 mm (depending on location). The flooding in early April 2010 was precipitated by 288 mm of rainfall in a 24-hour period. These floods were associated with a weak El Niño event, but the floods in early 2011 were actually associated with a La Niña event, so the linkage is not consistent.[iv]

Rio's peculiar physical setting, and the circumscribed nature of suitable building sites, has spawned two kinds of response. One is the construction of high-rise apartments close to the coastline (e.g., Copacabana, Ipanema and Leblon) and in flood-prone areas further inland; the other is unregulated construction on steep slopes, particularly on the Tijuca mountain range. The unregulated construction of *favelas* (shanty towns) has a long history, and stems from the invasion of both private and public urban lands by poor urban squatters who become de facto (and in some cases de jure) owners of plots of land.[v]

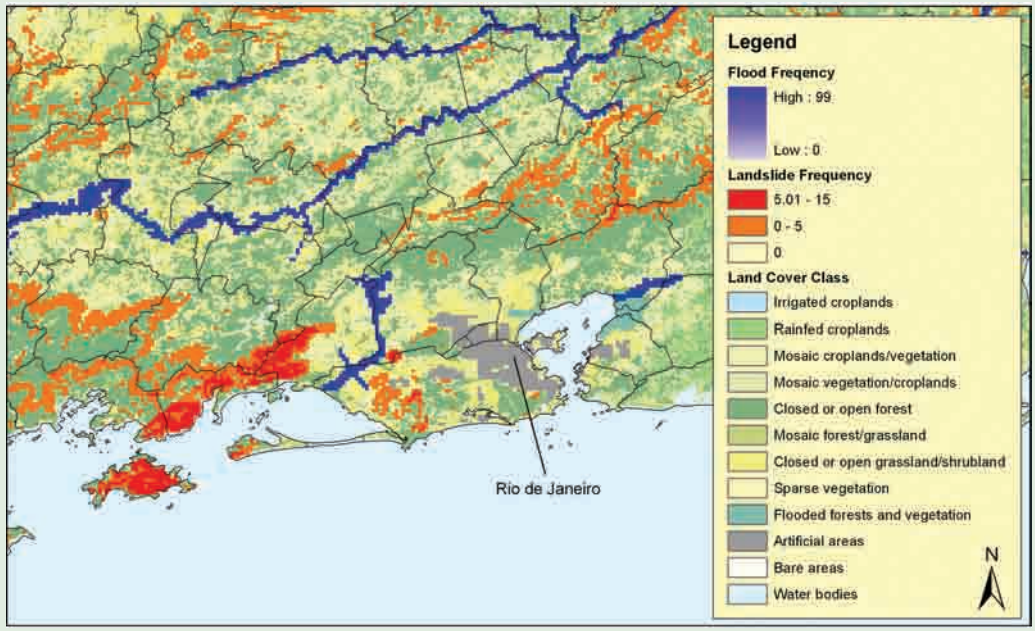

Box Figure 3.1: *Rio de Janeiro: flood and landside risk (Global Risk Data Platform Preview). Flood frequency is the expected average number of events per 100 years. Landslide frequency is the expected annual probability and percentage of pixel of occurrence of a potentially destructive landslide event ×1,000,000.*

Sources: UNEP/DEWA/GRID-Europe. 2009. Flood frequency. In: ISDR (2009) Global Assessment Report on Disaster Risk Reduction. United Nations, Geneva, Switzerland; International Centre for Geohazards (NGI). 2009. Frequency of landslides triggered by precipitations. In: ISDR (2009) Global Assessment Report on Disaster Risk Reduction. United Nations, Geneva, Switzerland; European Space Agency. 2009. Globcover for South America (global legend).

In terms of human vulnerability, Rio's income distribution is highly skewed. The existence of pockets of extreme poverty side-by-side with affluent neighborhoods is characteristic of the city. The 2000 census reported that 1.1 million people live in *favelas*, or 20 percent of the municipality's population. The city is also densely settled: the municipality has an average density of 4,640 persons per sq km but densities in the smaller administrative units of the metro area are between 8,000 and 12,000 persons per sq km.

Rio has a large migrant population from the poorest parts of Brazil's arid northeast region. The fact that many of them do not have personal experience with mudslides or mass wasting may account for their building practices. Migrants move up hillsides in search of new land, consistently eating away at the vegetation cover on the slopes above the *favelas*, despite government efforts to cordon off such areas to prevent further development. New regulations have been put in place that restrict building in hazard-prone areas. Efforts to "regularize" *favelas* have also been underway for several years, with various government programs to undertake cadastral surveys, grant deeds to de facto owners and provide basic infrastructure. These same plans limit the further expansion of *favelas* in flood-prone or steeply sloped areas. Rio de Janeiro has invested more than US$600 million in its *Programa Favela Bairro* to improve access to basic infrastructure, health and education for half a million of its poorest residents.[vi] In terms of social cohesion, the *favelas* do have some rudimentary organization, including neighborhood watches and self-improvement societies. These can be important for self-help and early warning systems. The drug traffic entrenched in many *favelas* (and the violence it spawns) is a major counter-force to these elements – a problem that has no end in sight.

Although *favelas* have always suffered during rainy seasons, the development up slope and paving of walkways has had the effect of increasing runoff to the low-lying areas. Runoff is channeled down cemented and quasi-natural watercourses to the narrow coastal lowlands, where they join canals whose limited flow capacity causes frequent flooding. By contrast, the Baixada Fluminense, a large marshy lowland somewhat removed from the steeper parts of the city, has had reasonably adequate drainage since the 1930s.[vii]

Generally, precipitation extremes are expected to increase in severity with climatic change, and these will have adverse impacts on Rio, given that the city already experiences extreme flooding and landslides on a roughly 20 year basis. Poor neighborhoods are particularly vulnerable to this extreme precipitation: roughly 300 people died and more than 20,000 people were made homeless during a 1967 flood, and in 2010 the Morro do Bumba slum built on a former garbage dump in Niteroi collapsed and slid downhill, burying homes and killing more than 200 people. Extreme and unpredictable rainfalls and floods converge with projected sea-level rise to increase stresses that will be difficult for Rio to handle owing to the city's topography (narrow coastal shelf backed by steep mountains subject to mass erosion), poor building conditions, the lack of secure land tenure for a notable portion of the city's population, poverty coupled with large income inequalities, and large problems with sanitation systems and sewage disposal.

Little in the way of concrete flood protection infrastructure has been set up in the wake of the 1988 floods. It is possible to speak of highly vulnerable sub-populations living in *favelas* and near waterways, and relatively less vulnerable upper classes living in high-rise apartments in locations less susceptible to inundation. This speaks to the need to upgrade slums, limit settlement on steep slopes and unstable locations, relocate some settlers on some slopes, revegetate hillsides, create more green verges near waterways for water absorption, and improve drainage systems in low-lying areas. Part of this will entail cleaning and maintenance of existing waterways and canals. A number of more specific suggestions for climate proofing are provided in the volume by Gusmão *et al*. (2008).

[i]This is dedicated to Daniel J. Hogan, who passed away in 2010. Dan was a leader in the field of population-environment studies and did much work on urbanization impacts on the environment in Brazil.

[ii]"April 2010 Rio de Janeiro floods and mudslides", Wikipedia, accessed on January 19, 2011 at http://en.wikipedia.org/wiki/April_2010_Rio_de_Janeiro_floods_and_mudslides; "Brazil mudslide death toll passes 450", CBC News, accessed on January 20, 2011 at http://www.cbc.ca/world/story/2011/01/13/brazil-flood-deaths.html.

[iii]Gusmão, P. P., P. Serrano do Carmo, and S. B. Vianna (2008). *Rio Proximos 100 Anos*. Rio De Janiero: Instituto Municipal de Urbanismo Pereira Passos.

[iv]National Weather Service's Climate Prediction Center for a list of El Niño and La Niña years, accessed on January 20, 2011 at http://www.cpc.ncep.noaa.gov/products/analysis_monitoring/ensostuff/ensoyears.shtml.

[v]Fernandes, E. (2000). The legalisation of *favelas* in Brazil: problems and prospects, *Third World Planning Review,* **22** (2), 167–188.

[vi]UN HABITAT (2006). *State of the World's Cities*, London, UK: Earthscan.

[vii]Cunha, L. R. and M. Miller Santos (1993) The Rio reconstruction project: the first two years. In *Towards A Sustainable Urban Environment: The Rio de Janeiro Study*, World Bank Discussion Paper 195, Washington, DC, USA: World Bank.

3.2.1.1 São Paulo and the El Niño–Southern Oscillation

The ENSO can have a strong effect on rainfall in São Paulo, Brazil, although this city is situated between regions of opposite effects of ENSO in the rainy season, Central-East and South Brazil. In Central-East, ENSO affects the frequency of extreme daily precipitation events in opposite wasy in the early and peak summer rainy season (Grimm and Tedeschi, 2009). In São Paulo, the behavior is different: there is significant impact in the early rainy season (October–November) but no consistent impact in the peak rainy season (January–February). Enhanced precipitation in the early rainy season, which is more frequent during El Niño episodes, can have a significant impact, since in this case urban floods and landslides may become more frequent during the rainy season. Flooding and landslides are disruptive, costly, and deadly.

3.2.2 Effects of the North Atlantic Oscillation on cities

The North Atlantic Oscillation (NAO) is the dominant pattern of atmospheric circulation variability in the North Atlantic region

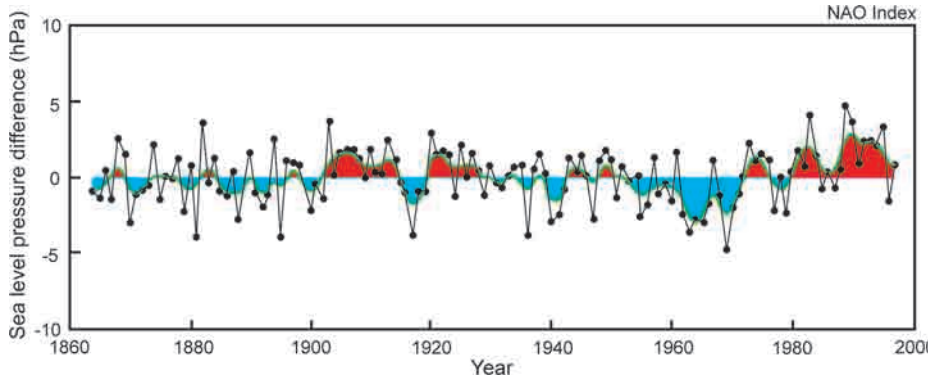

Figure 3.8: *NAO Index. One measure of the NAO Index is the difference in sea level pressure between the polar low near Iceland and the subtropical high near the Azores. Red indicates the positive phase of the NAO and blue indicates the negative phase of the NAO.*

Source: Hurrell (1995), with data from NCAR.

(Hurrell *et al.*, 2003). Although concentrated there, the impacts on climate extend over cities in a much larger region, from central North America to Europe, Asia, and Africa. When the NAO index is positive, there is a higher than usual subtropical high pressure (located in the general area spanning Portugal and the Azores) and a deeper than normal Iceland low pressure (Visbeck *et al.*, 2001; Figure 3.8) This larger pressure difference produces stronger-than-average westerly winds at middle latitudes, resulting in warm and wet winters in eastern USA and most of Europe and cold and dry winters in Canada and Greenland. Drier and colder conditions also prevail over southern Europe, the Mediterranean, and northern Africa. The oscillation and its aforementioned impacts are strongest in winter, but are present throughout the year. The NAO index varies from month to month and from year to year; however, the long-term average tends to remain in one phase for multi-year periods.

The negative NAO index refers to a weaker and eastward-displaced subtropical high, and a weaker Iceland low, leading to anomalies that are largely opposite of those associated with the positive NAO index. The mid-latitude winds are weaker and in a more west–east direction during negative NAO events. Warm and moist air is brought into southern Europe and cold temperatures prevail in northern Europe and in eastern USA. Canada and Greenland experience higher winter temperatures.

The impacts of NAO on precipitation and temperature in North America and Europe have urban consequences for hydropower generation (through water availability), energy consumption (through temperatures and humidity), water supply, and ecosystems (drought and forest fires, for example) among other sectors. Cities highlighted in this chapter that are impacted by the NAO include New York City, Toronto, London, and Athens. A London example is presented below.

3.2.2.1 London and the North Atlantic Oscillation

One city featured in this chapter that is affected by the NAO is London. Changes in the phase of the NAO have an impact on temperature and precipitation in the city, especially during the wintertime. The general relationship between the phase of the NAO and climate in London is that the positive phase brings wetter and warmer conditions, while the negative phase brings drier and colder conditions (Wilby *et al.*, 1997). In early 2009, London experienced a rare heavy snowfall, which crippled the transportation system and forced many businesses to close. At that time, the NAO was in the negative phase, which helped transport cold air to the city. The snowfall in 2009 is an example of how expected relationships of natural climate variability do not always hold. While the colder temperatures were typical for the negative NAO, the increased precipitation was not.

3.2.3 Other modes of natural climate variability

In addition to ENSO and the NAO, there are other modes of natural climate variability that impact cities. These include the Pacific Decadal Oscillation (PDO), the Southern Annular Mode (SAM), the Atlantic Multidecadal Oscillation (AMO), the Indian Ocean Dipole (IOD), and the Madden–Julian Oscillation (MJO). The PDO is a longer timescale (decadal compared to inter-annual) pattern of variability that affects the climate in the Pacific Basin. The SAM is a mode of extra-tropical variability in the Southern Hemisphere that affects the climate in South America and Australia. The AMO is a mode of natural variability of North Atlantic Ocean sea-surface temperatures that influences Atlantic Basin hurricane activity. The Indian Ocean Dipole (IOD) is a coupled ocean–atmospheric mode centered on the tropical Indian Ocean Basin. The Madden–Julian Oscillation is an intra-seasonal mode of variability that primarily influences precipitation in the tropics.

3.2.4 Natural variability and global climate change

The frequency and intensity of the modes of natural climate variability and their associated teleconnections may change with global climate change. Because of the non-linearity of the climate system, it is not possible to simply add the teleconnections of a particular mode to a changing background climate (Hoerling *et al.*, 1997). It is important to analyze long-term observations of the modes to learn how they have varied in the past and if they are exhibiting any trends in the current climate. Climate change and climate variability may interact in complex and unpredictable

ways. For example, shifts in mean wind patterns (such as the jet stream) associated with climate change may modify the regional teleconnections of the modes. It is possible that the accuracy of seasonal forecasts may change in some regions as climate change accelerates.

There remains much uncertainty as to how El Niño/La Niña conditions may change with a warmer climate. While some studies suggest that with increased greenhouse gas concentrations, the El Niño pattern may become more dominant, there is great uncertainty surrounding this issue (Collins, 2005).

For the NAO, some scientific evidence including modeling studies suggests that, with a warmer atmosphere, ocean temperatures will rise in a pattern that reinforces the positive phase of the NAO. As was the case with projections of ENSO with global warming, future patterns of the NAO also remain extremely uncertain (Visbeck *et al.*, 2001).

3.3 Global climate change and its impact on urban areas

Along with all other planetary surfaces, urban climates are subject to global changes due to radiative forcing. The impact of global change on cities is the subject of this section.

3.3.1 The climate system and global climate change

The elements of the global climate system include the atmosphere, biosphere, hydrosphere, cryosphere, and lithosphere (Figure 3.9). The climate system is coupled, in the sense that the components interact at many spatial and temporal scales.

The Earth's climate is determined by the long-term balance between incoming solar radiation and outgoing terrestrial radiation. Incoming solar radiation is partly absorbed, partly scattered, and partly reflected by gases in the atmosphere, by aerosols, and by clouds. Under equilibrium conditions, there is an energy balance between the outgoing terrestrial or "longwave" radiation and the incoming solar or "shortwave" radiation. Greenhouse gases are responsible for an approximately 30 °C elevation of global average surface temperature. Since the Industrial Revolution, increasing greenhouse gas concentrations due to fossil fuel combustion, cement-making, and land use changes has increased the mean surface temperature of the Earth by approximately an additional 1 °C.

These and other climate changes and impacts have been documented by an international panel of leading climate scientists, the Intergovernmental Panel on Climate Change (IPCC), formed in 1988 to provide objective and up-to-date information regarding the changing climate. Key findings of the 2007 Fourth

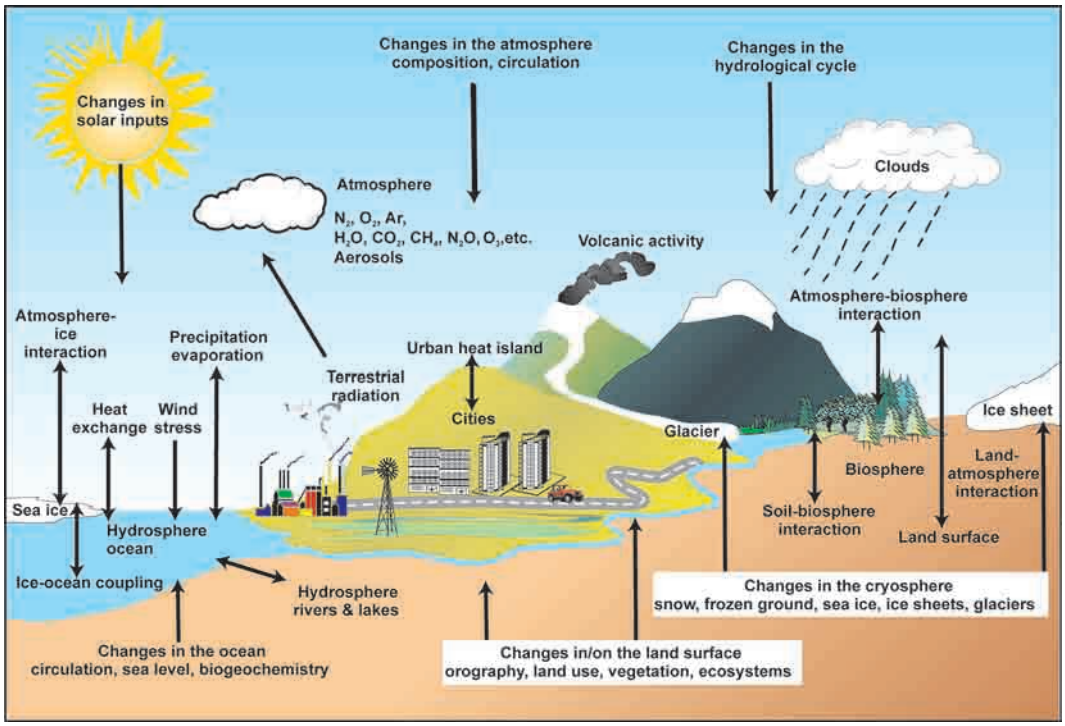

Figure 3.9: *The global climate system. Shown are the many interactions among the different components of the climate system, which includes cities.*

Source: IPCC, WGI (2007).

Assessment Report (AR4; IPCC, 2007) included the following (as summarized in Horton *et al*., 2010):

- there is a greater than 90 percent chance that warming temperatures are *primarily* due to human activities (IPCC, 2007);
- atmospheric concentrations of carbon dioxide (CO_2) are now more than one-third higher than pre-industrial levels;
- concentrations of other important greenhouse gases methane (CH_4) and nitrous oxide (N_2O) have increased by more than 100 percent and close to 20 percent respectively over the same time period;
- further increases in greenhouse gas concentrations are projected to lead to further temperature increases and associated changes in the climate system;
- over the twenty-first century, global average temperature is expected to increase by between 1.8 and 4.0 °C.

Warming is expected to be largest over land and in the high-latitude North, where some Arctic cities may experience warming exceeding 8 °C by 2100. Outside the tropics and subtropics, the largest warming is generally expected in winter. Generally speaking, precipitation is expected to increase in high-latitude cities and decrease in subtropical cities. Hot extremes and cold extremes in cities are generally expected to increase and decrease respectively.

As CO_2 continues to be absorbed by the oceans, ocean acidification will accelerate, with potentially large implications on marine ecosystems. While the implications may be largest for those coastal cities where marine ecosystems are a source of economic livelihood and sustenance, in a global economy all the world's cities would be indirectly impacted by large-scale ocean acidification.

3.3.2 Drivers of global climate change

The global changes described above can largely be attributed to three drivers, or causes, of climate change: greenhouse gases, aerosols, and land use changes. These three drivers, with emphasis on urban contributions, are described below.

3.3.2.1 Greenhouse gases

Gases that trap heat in the atmosphere are referred to as greenhouse gases. Three primary greenhouse gases that are directly linked to anthropogenic activities are carbon dioxide (CO_2), methane (CH_4), and nitrous oxide (N_2O). As centers of population, economic activity, and energy use, cities are responsible for a large portion of greenhouse gas emissions. On a per capita basis, however, urban residents in developed nations probably have lower emission rates than ex-urban residents due to the inherent energy efficiencies of mass transit and multiple-resident buildings.

Some greenhouse gases, such as carbon dioxide, occur in the atmosphere through natural processes, while others, such as the hydrofluorocarbons, are created solely from human activities. Carbon dioxide, which accounts for over 75 percent of all greenhouse gas emissions, is emitted into the atmosphere through the burning of fossil fuels and the clearing of land for agriculture. Methane is emitted from natural gas production, livestock, and agricultural production. Application of nitrogen fertilizer for agricultural production also leads to nitrous oxide being emitted into the atmosphere. Most hydrofluorocarbons, another important greenhouse gas, come from industrial activity.

3.3.2.2 Aerosols

Aerosols are atmospheric particles of both natural and anthropogenic origin. Natural aerosol sources include volcanoes and sea salt, while key anthropogenic sources include fossil fuel combustion and biomass burning. Aerosol concentrations tend to be higher in urban than rural areas, although during times of extensive biomass burning rural areas can have comparable concentrations. Climatic, human health, and visibility effects of aerosols have been documented. (Shu *et al*., 2000, 2001; Pawan *et al*., 2006; Eri *et al*., 2009). Aerosols modify the earth's energy budget by scattering and absorbing short- and longwave radiation. As a prime radiative forcer (Charlson *et al.*, 1992), aerosol particles also influence cloud optical properties, cloud water content, and lifetime. That is referred to as the indirect effect of aerosols, or indirect climate forcing (Harshvardhan, 2002). Volcanic aerosols can lead to brief periods of global cooling, and biomass burning of agricultural regions has been shown to affect regional weather. While greenhouse gas effects are primarily global and regional in scale, aerosol effects span from the global to the urban scale.

3.3.2.3 Land use change

Land use change and urbanization influence the climate through changes in surface albedo, land roughness, hydrological and thermal features. Across the globe, human activities have changed the face of the planet. Deforestation has modified the climate by changing solar absorption and moisture transfer rates, as well as increasing carbon dioxide levels. Agricultural expansion has modified these processes as well. Urbanization and development have led to decreased groundwater absorption by the land and more heat absorption as the built environment expands (Zheng *et al*., 2002; Gao *et al*., 2003; Pielke, 2005; Lian and Shu, 2007). Like aerosol effects, the climatic effects of land use changes range from large regional scales to urban scales.

3.4 Observed climate change in cities

We present observed long-term climate data for the 12 cities to evaluate whether there are long-term trends. The urban heat island effect that may exist in each case should in principle be captured by the urban weather stations used. The selected cities include a wide range of climate zones. Tropical cities such as Dakar are characterized by warm temperatures throughout the year. The mid-latitude cities, in contrast, all experience a continental climate,

with large temperature differences between summer and winter seasons. Some cities such as Delhi have a monsoonal climate, with the majority of the precipitation occurring during one part of the year, while other cities such as New York experience substantial precipitation during all months. These differences in background climate can be thought of as the foundation for the unique blend of climate change hazards each city faces, since climate changes are superimposed on a city's baseline climate.

Over the past century, there have been significant observed trends in climate hazards including annual mean temperature, annual precipitation, and extreme events, such as heat waves and intense precipitation, at global scales (IPCC, 2007). Trend analyses are a first step towards attributing changes to factors ranging from variability to greenhouse gases, to changes in the urban environment.

The observed annual temperature and precipitation values for each city were computed using a monthly data set.[1] The months in the data set that were missing were replaced by the climatological average for that month over the full time series for the city. The period over which the observed trends were analyzed was 1900 to 2005 unless otherwise noted. For the temperature trends, the following cities did not have data sets running the entire length of this period; Toronto (1938–2005), Delhi (1931–2005), Kingston (1943–2005), and Harare (1900–2002). For the precipitation trends, Toronto (1938–2005) and Harare (1937–2002). A brief city-by-city summary for observed trends in temperature and precipitation is shown in Table 3.2. The statistical significance of the trends is also included. Graphs of the observed climate data for each of the 12 cities are shown in Figure 3.10.

3.4.1 Temperature

Observations of annual mean temperature are used to determine whether or not a city is experiencing warming or cooling. In addition to mean temperature, maximum temperature and minimum temperature can also be used to identify changes in the climate. For these variables, finer temporal scales (daily data) are useful for analysis of observed climate trends. However, because of the limited data records for some cities, obtaining climate data on these small timescales can be difficult. These additional temperature variables can also be used in the analysis of extreme climate events, including hot days and heat waves.

For the 12 cities that were selected for the chapter, observed trends in annual mean temperature showed warming in 10 of the cities. Over the past century the most rapid rate of warming has occurred in São Paulo. The city had a trend of +0.27 °C per decade. The two cities that showed cooling (temperatures decreasing over the time period) were in Africa. Dakar and Harare had observed trends in annual mean temperature of –0.09 °C and –0.06 °C respectively. However, for these two cities, while the overall trend is negative, both have seen warming in the past two decades.

Table 3.2: *Observed climate trends in cities.*

City	Years	Number of missing months	Temperature trend (°C per decade)
Athens	1900–2005	15	0.03
Dakar	1900–2005	57	–0.09**
Delhi	1931–2005	10	0.03
Harare	1900–2002	44	–0.06**
Kingston	1943–2005	59	0.19**
London	1900–2005	0	0.08**
Melbourne	1900–2005	0	0.14**
New York	1900–2005	0	0.16**
São Paulo	1900–2005	30	0.27**
Shanghai	1900–2005	33	0.05**
Tokyo	1900–2005	2	0.26**
Toronto	1938–2005	4	0.10
City	**Years**	**Number of missing months**	**Precipitation trend (mm per decade)**
Athens	1900–2005	11	2
Dakar	1900–2005	24	–20**
Delhi	1900–2005	18	16*
Harare	1937–2002	26	–21
Kingston	1900–2005	19	–15
London	1900–2005	0	2
Melbourne	1900–2005	0	–4
New York	1900–2005	0	18
São Paulo	1900–2005	16	29**
Shanghai	1900–2005	24	–3
Tokyo	1900–2005	2	–17*
Toronto	1938–2005	4	7

Annual temperature and precipitation statistics are computed for all cities using data from the National Climatic Data Center Global Historical Climatology Network (NCDC GHCN v2), UK Met Office and Hadley Centre, Australian Bureau of Meteorology, and Environment Canada.

The single star (*) indicates that the trend is significant at the 95 percent level and the double star (**) indicates that trend is significant at the 99 percent level.

Although most of the cities did show a warming trend, the trends in each individual city vary by their rate of change. For example, one city may have had a slow increase for a large part of the twentieth century with a rapid warm up at the end of the period, while another may have seen a moderate increase over the entire time period. Further investigation of the trend for each individual city is necessary to understand the possible causes and potential impacts of warming temperatures. The rate at

1 For data sources, see Table 3.2

which the urban heat island is increasing in each city will affect observed temperature trends. For example, approximately one-third of the warming trend in New York City has been attributed to urban heat island intensification (Gaffin *et al.*, 2008). In developing countries, the rate is probably higher (Ren *et al.*, 2007).

3.4.1.1 Tokyo's heat island

As temperatures rise in Tokyo, residents are experiencing more health problems, including heatstroke and sleeping difficulties. Both are associated with higher nighttime temperatures (Figure 3.11).

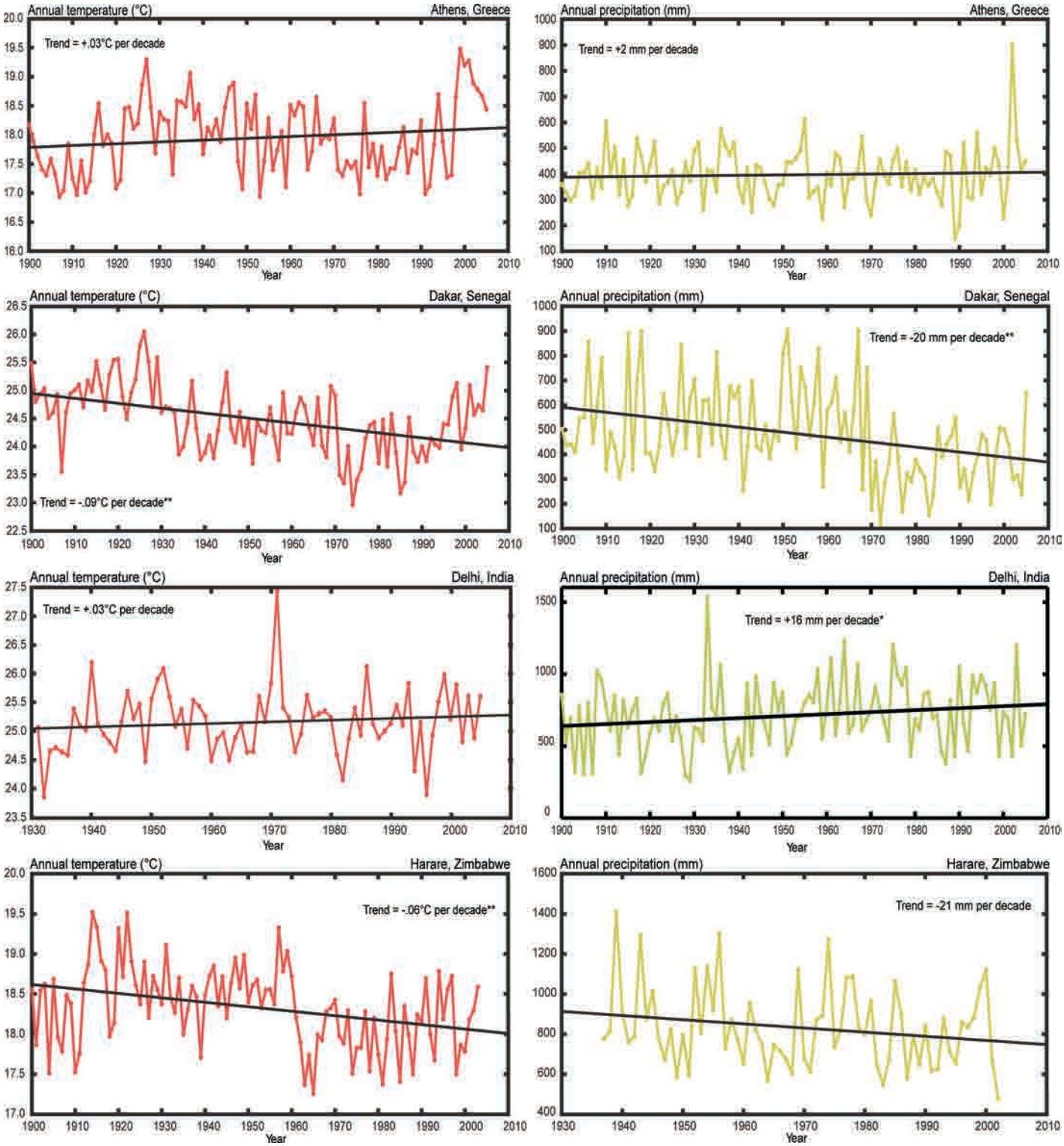

Figure 3.10: *Observed climate trends in cities. Trends and statistical significance are shown for the data available for the twentieth century (see Table 3.2 for specific years for each city). Note differences in temperature and precipitation scales.*

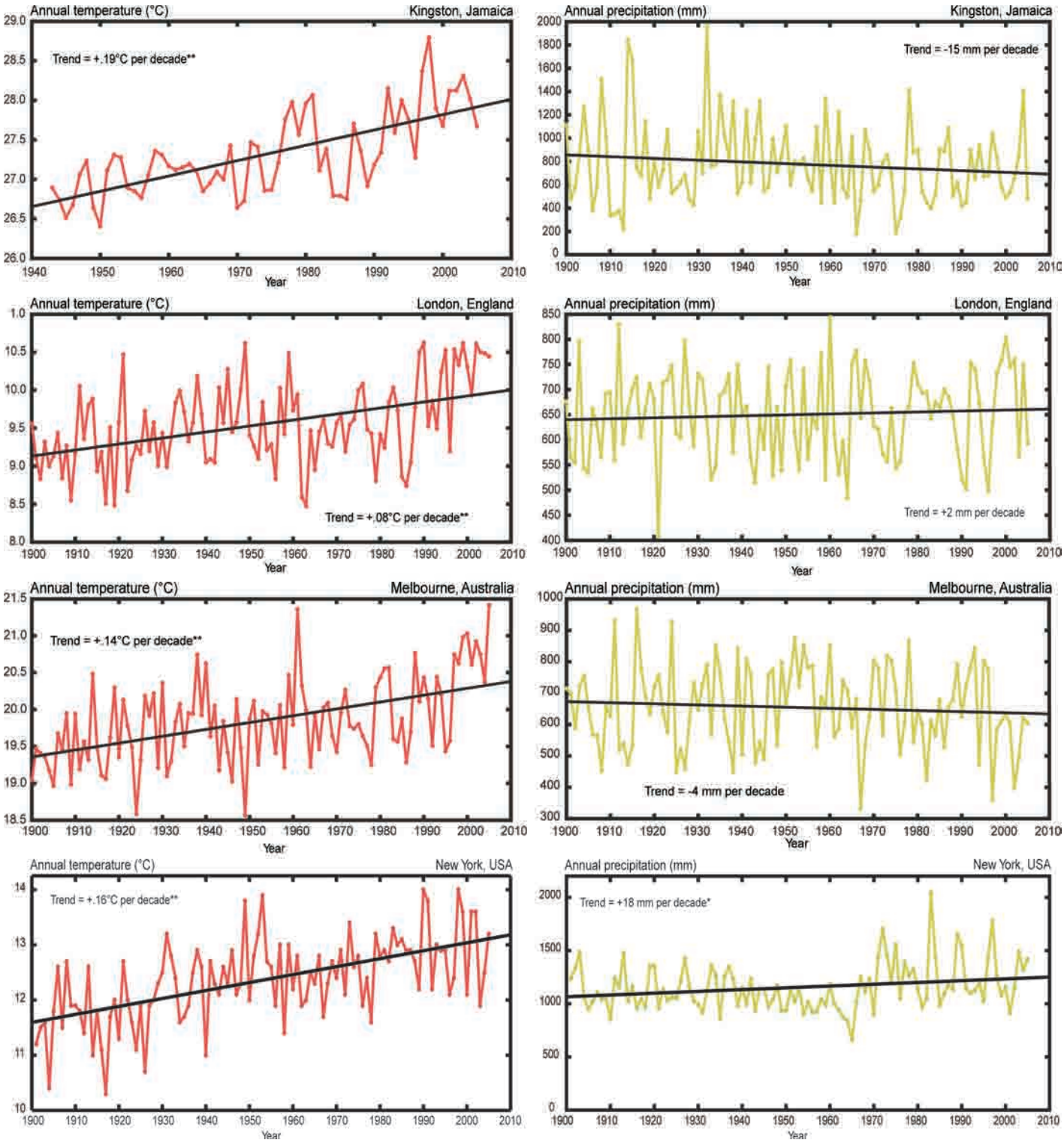

Figure 3.10: *(continued)*

Additional impacts include ecosystem changes such as earlier flowering dates and changes in insect and amphibian populations.

3.4.1.2 Observed temperature trend in São Paulo, Brazil

For the cities chosen for the chapter, São Paulo had the most rapid rate of increase in mean annual temperature. Over the period from 1900 to 2005, mean temperature in the city rose at a rate of 0.27 °C per decade. Much of the warming is occurring at night, with minimum temperature increasing at a faster rate than maximum temperature. The average of these two variables, maximum and minimum temperatures, is the mean temperature. São Paulo's warming was greater in winter than in summer. Some of the warming in São Paulo may be

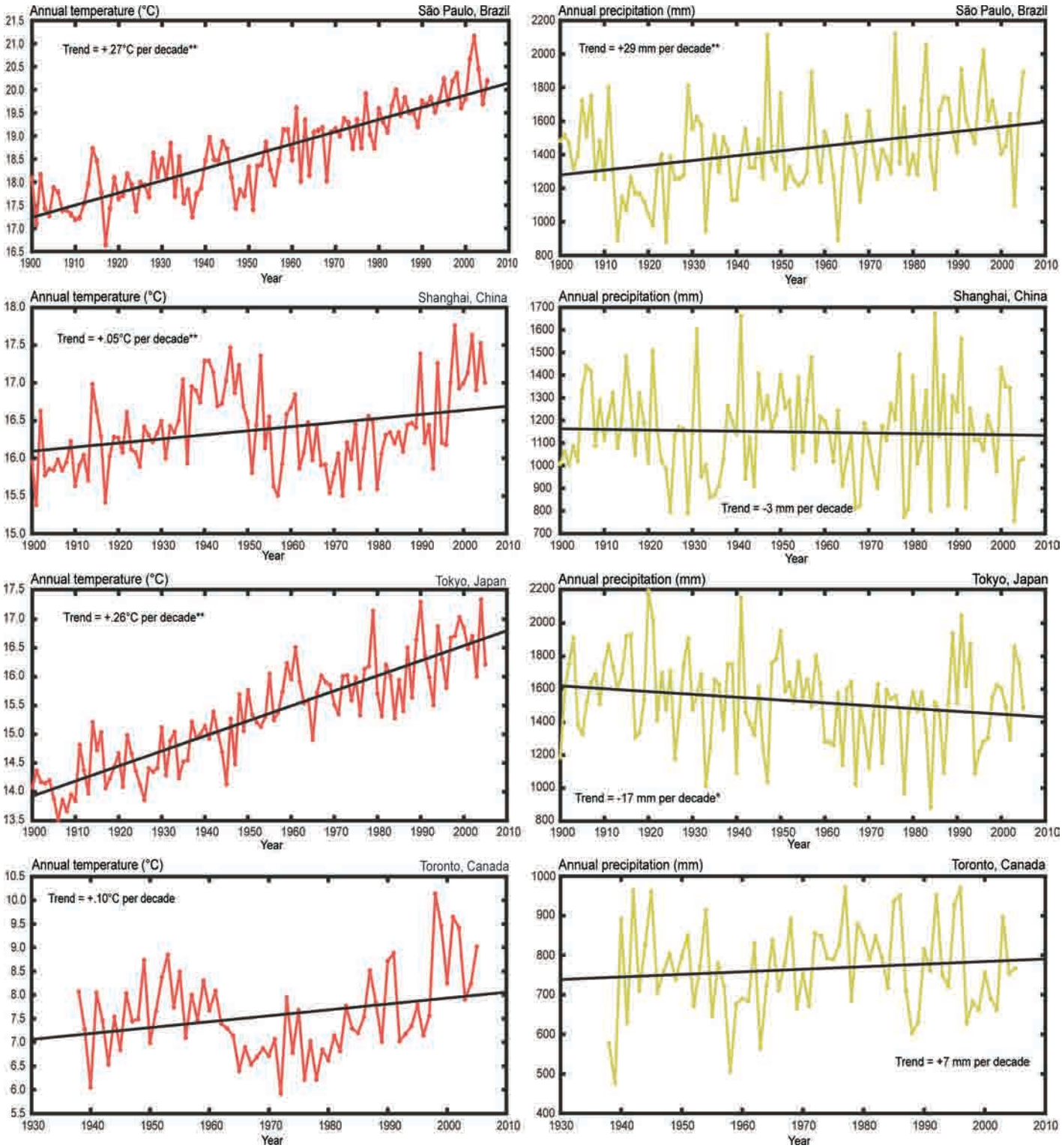

Figure 3.10: *(continued)*

caused by land use changes due to urbanization (Marengo and Camargo, 2008).

The observed warming in mean annual temperature appears to be greatest over approximately the past 20 years, as compared to the 20 years prior to that. Some of this variation between time slices can be explained by changes in the frequency of modes of natural climate variability. ENSO events in recent years coincide with the more rapid rates of warming. In addition, warming temperatures in the South Atlantic Ocean also may influence the warming mean temperatures in São Paulo (Marengo and Camargo, 2008).

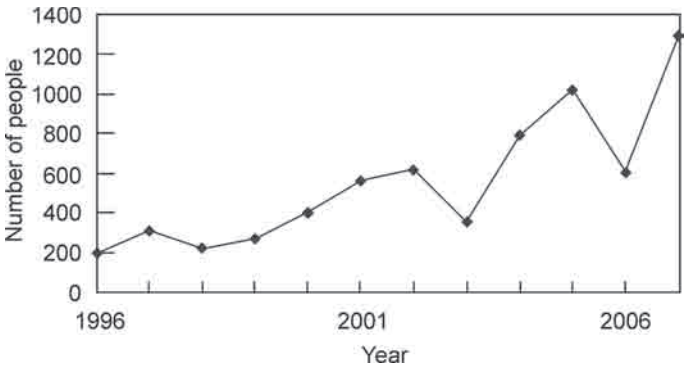

Figure 3.11: *Urban heat island impacts in Tokyo, Japan. The number of people sent to the hospital with heatstroke has been increasing over time.*

Source: Tokyo Metropolitan Government

3.4.2 Precipitation

Observations of annual total precipitation reveal precipitation changes in cities on decadal timescales. Natural climate variability can greatly influence annual precipitation (more so than temperature). Changes in the inter-annual variability of precipitation can also provide insight into how the climate is changing. For example, in New York City, while annual precipitation has only increased slightly in the past century, inter-annual variability has become more pronounced. In addition, analyzing trends in monthly rainfall can also be useful, as many cities experience two distinct seasons, such as the monsoons in Delhi, India. Data on shorter timescales, such as daily and weekly, can be used in extreme events analysis of droughts, floods, and intense precipitation rates. Again, with limited data records for some cities, obtaining climate data on these small timescales can be difficult.

Precipitation trends for the 12 cities reflect the regional nature of precipitation changes with climate change, relative to the largely homogenous changes expected in temperature. Of the 12 cities looked at in the chapter, half saw increasing trends in annual precipitation. Over the past century the most rapid rate of precipitation increase has occurred in São Paulo (+29 mm per decade), and the largest decrease has occurred in Harare (–21 mm per decade).

For the cities where observed trends in annual precipitation showed increasing (decreasing) precipitation, the trends do not reveal whether the wetter (drier) conditions are caused by more (less) frequent heavy rainfall events or more (less) persistent lighter rainfall. Also, the direction of trends for extreme precipitation events, such as days where precipitation is greater than 50 mm, will not necessarily correspond to the trend in annual precipitation. For example, a city could experience a decreasing trend in annual precipitation, but have an increase in short-duration intense precipitation events.

As was the case with temperature, there are multidecadal fluctuations in observed precipitation trends specific to each city. This is especially true for this climate variable given the large

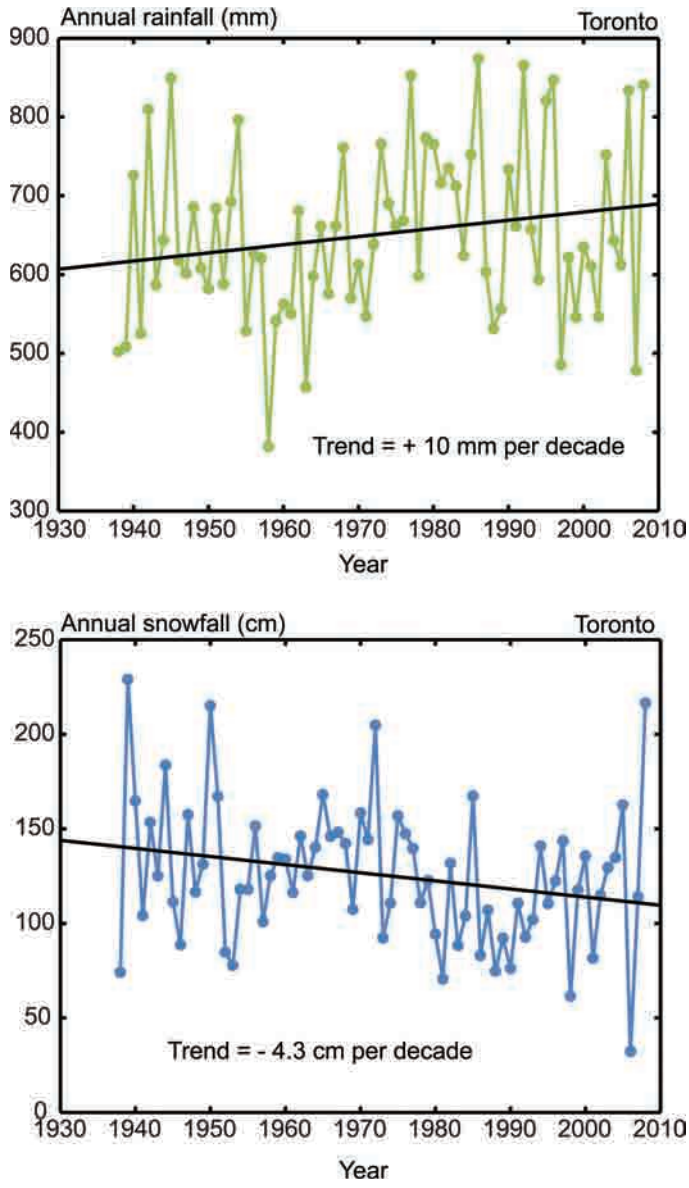

Figure 3.12: *Observed precipitation trends from 1938 to 2005 in Toronto, Canada: rain above; snow below. Showfall trend is significant at the 95% level.*

Source: Data are from Environment Canada.

inter-annual variability of precipitation. Cities with increasing annual precipitation over the time period still may have pronounced periods of drought, while those experiencing a drying trend may still have years with higher than average rainfall.

3.4.2.1 Observed precipitation trend in Toronto, Canada

Toronto is one city selected for this chapter that receives precipitation in the form of snow. While total precipitation has been increasing over the past century in the city, most of the increase has been in the form of more rainfall. Snowfall in Toronto has been on the decline, leading to a decrease in the percentage of total precipitation falling as snow. The trends for observed annual rainfall and snowfall in Toronto are presented in Figure 3.12, with rainfall and snowfall shown in green and blue respectively. Rainfall

has increased at a rate of 10 mm per decade while snowfall has decreased at a rate of 4.3 cm per decade between 1938 and 2008.

To some extent, trends in precipitation for a given city depend on annual mean temperatures. In a warmer climate, the atmosphere can hold more moisture, allowing for more precipitation. But higher temperatures also can alter the type of precipitation that will fall. For Toronto, warmer temperatures have allowed for more precipitation; in the spring, precipitation that once fell as snow is now falling as rain. This trend is not evident in many of the colder parts of Canada. In colder areas the increases in total annual precipitation (like those observed in Toronto) have included increases in snowfall, especially during the winter months. Temperatures in these areas of the country have warmed enough to allow for more precipitation but have not crossed the threshold for snow to become rain (Zhang *et al.*, 2000).

3.4.3 Sea level rise

Sea level rise analysis was not performed for all of the coastal cities due to limited data sets. However, coastal cities are extremely vulnerable to rising sea levels, since approximately 35 percent of world population lives within 100 km of the coast (Hachadoorian *et al.*, 2011; L. Hachadoorian, pers. comm.).

[ADAPTATION] Box 3.2 Sorsogon City, Philippines, responding to climate change

Bernhard Barth and Laids Mamonong

UN-HABITAT

Sorsogon City is one of 120 cities in the Philippines in the Asia Pacific region. It has a land area of 313 square kilometers with a population of 151,454 (as of 2007) growing at a rate of 1.78 percent annually. Its economy is based mainly on agriculture, fishing, trade, and services. It is the capital and the administrative, commercial, and educational center of Sorsogon Province.

In August 2008 the city launched a Climate Change Initiative, championed by the new mayor. Until then the popular perception was that climate change is a global and national issue requiring limited action from the local government. A series of briefings for decision-makers and local leaders was conducted to enhance basic understanding of climate change and the important role of local government. This resulted in an expressed commitment from decision-makers in developing their city's climate change profile and defining responsive local actions.

Various city stakeholders worked together with the local government in the conduct of a participatory vulnerability and adaptation (V&A) assessment. Using climate change projections and risk assessments from national government agencies and private research institutions, the city government developed its local vulnerability assumptions. To assess local impacts, the city gathered and analyzed its own recorded observations. These were further substantiated by local people's accounts of their personal experiences. During city consultations, residents recounted how typhoons and storm surges over the past decade had become stronger and more destructive. These records and personal accounts were recorded as evidence of climate change impacts through community risk mapping. Using hand-drawn maps, local people graphically described the changes in the reach of tidal flooding and identified the areas gradually lost due to sea level rise and erosion. This participatory exercise promoted ownership by the locals of the assessment process and results, and increased their awareness of climate change impacts. Moreover, the process empowered the people to work together with the local government in finding practical solutions that they can personally act on.

As noted in the city's climate change profile, the city was badly hit by two super-typhoons in 2006, causing widespread devastation within a two-month interval and leaving in their wake a total of 27,101 families affected and 10,070 totally damaged houses (Box Figure 3.2). The first typhoon, in just 5 hours, caused damage to public infrastructure estimated at 208 million pesos or US$4.3 million. The city is projected to experience more cases of prolonged monsoon rains resulting in total rainfall exceeding 2,800 to 3,500 mm per year.

The V&A assessment revealed that the city's geographical location and previous stresses make it sensitive to changes in extremes – such as tropical cyclones, storm surges, and extreme rainfall/flooding – and changes in means – such as increased temperature, increased precipitation, and sea level rise. With sea level rise projected to accelerate, the city's built-up areas situated near the coast present the highest vulnerability to climate change impacts because they have the highest concentration of people, especially informal settlers, living in inadequate structures in danger zones. These areas are also the hub for economic activities (accounting for 60 percent of the economy) and the location of basic lifelines such as water, electricity, and basic service facilities. Around 36 percent of the total population, or 55,000 people, are vulnerable to flooding. Over 35,000 people from nine coastal villages are threatened by sea level rise and storm surge, of whom 22,000 are women.

Box Figure 3.2: *Section of seawall in Beacon District, Sorgoson, partially destroyed by a 2006 storm. Many of Sorgoson's informal settlements are just behind the seawall.*

Source: UN-HABITAT/Bemhard Barth

Knowing these climate change vulnerabilities (areas, population, economic activities, policy gaps), the city government is now engaging local communities and the private sector in climate change adaptation planning. Using tools from UN-HABITAT's Sustainable Cities Programme, the local government conducted multisector city consultations that resulted in the identification of four priority "quick-win" responses to increase people's resilience to climate change, namely: (i) improving settlements and basic infrastructure, (ii) enhancing livelihoods, (iii) developing climate and disaster risk management systems, and (iv) improving environmental management and climate change mitigation actions. Issue working groups composed of representatives from people's organizations, NGOs, private sector, and LGU were organized to develop the action agenda per "quick-win" area and ensure its implementation.

So far the following important lessons have been learned:

1. There is a need to promote and advocate awareness on climate change among the general public and stakeholders through various media and community activities. This would broaden/establish partnerships among the private, public, academic, civil society, and neighbourhood associations for convergence of efforts on adaptation and mitigation.
2. The city government's capacity must be developed to make it more responsive to increase its resilience to climate change impacts. A framework must be developed to help and guide the city in integrating climate change considerations in the land use and development plans. A stronger link with national climate change programs is critical especially in enhancing building code and land use planning parameters.
3. The city needs to learn from good practices by other cities. It should also share its own experience in engaging various stakeholders in defining a collective climate change action.
4. It is crucial for the business sector to play a vital role in providing green building technology development and in promoting risk-resilient communities through the use of appropriate and innovative technologies in housing and infrastructure development.

The above lessons have become major considerations as the city works on mainstreaming climate change risk management into its local governance processes and implementing local climate change adaptation actions.

Source: UN-HABITAT (2010). Sorsogon City Climate Change Vulnerability and Adaptation Assessment. Available at: http:www.unhabitat.org.ph/climate-change/knowledge-productsoulputs.

Cities in this chapter at risk of sea level rise include New York, São Paulo, Tokyo, London, Shanghai, Melbourne, and Dakar. For all of these coastal cities, the sea level rise they are experiencing is caused by a combination of global and local factors. While the rate of sea level rise for each city due to global thermal expansion and meltwater from glaciers and ice sheets is the same, city-specific factors include land subsidence and local ocean height. These city-specific terms are necessary not only to determine the local rate of sea level and compare it to other cities and the global trend, but also for sea level projections.

3.4.3.1 Observed sea level rise in Dakar, Senegal

One city that is at risk of and has been experiencing rising sea levels over the past century is Dakar. Unfortunately, due to limited data availability, a common phenomenon in developing country cities, very little can be said about sea level rise trends. While sea level has been increasing at a rate of 1.5 cm per decade over the 11-year data record, for such short timescales natural variations and cycles can dominate any climate change signal. This example highlights the need for expanded data collection and quality control in many cities.

3.4.4 Extreme events

Extreme events can be defined as climate variables experienced in a limited duration. Temperature extremes include hot days where temperatures exceed a specified threshold, and heat waves–consecutive hot days. Precipitation extremes, which cover varying timescales, include intense/heavy precipitation events and droughts. Coastal storms and tropical cyclones are also types of climate extreme events.

Limited data availability at short timescales constrains analysis of urban extreme events. Extreme events also differ by city; for many inland locations, for example, coastal storm surges can be ignored. Some extreme events occur more frequently in association with certain phases of climate variability patterns such as ENSO. Because some variability patterns are somewhat predictable, there is an opportunity for seasonally forecasting these events, allowing cities to prepare for them in advance.

3.4.4.1 Hot days in Melbourne, Australia

One city that experiences hot days and heat waves is Melbourne. As defined by the World Meteorological Organization (WMO), hot days have maximum temperature exceeding 35 °C. For Melbourne, the trend from 1900 to 2008 shows no significant increase in the number of hot days, shown in Figure 3.13. The trend in hot days does not reveal a significant increase, even though annual average temperatures have risen significantly over the past century.

Combined with prolonged periods of dry weather, consecutive hot days (heat waves) have the potential to greatly impact cities and their surrounding areas. Specifically for Melbourne, years with above-average hot days, combined with other meteorological conditions, yield an increased threat of wildfires. Although the fires themselves are often in outlying areas away from the city, infrastructure, agriculture, ecosystems, water, and human resources critical to the city's survival may be impacted. Fires can also directly impact the city by reducing air quality. The most recent extreme warmth in early 2009, the heat wave of 2006, and in the summer of 1983 are all examples of years with increased fire activity and high numbers of hot days.

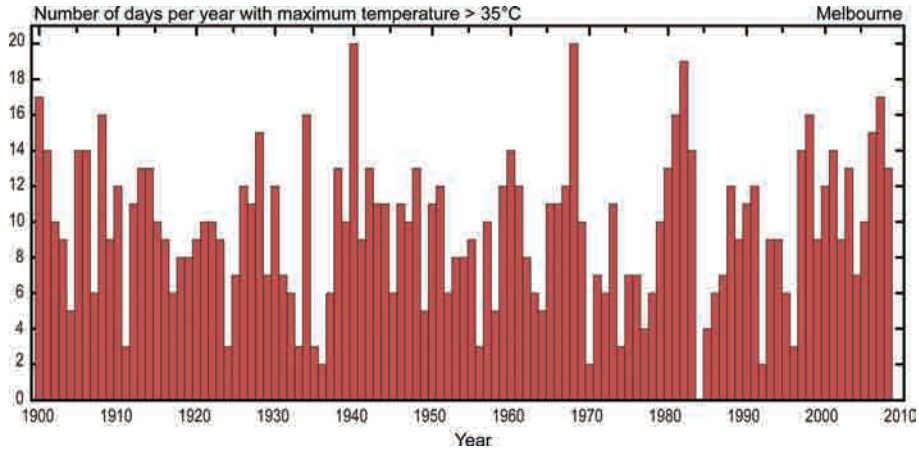

Figure 3.13: *Observed temperature extremes, hot days with temperatures above 35 °C, in Melbourne, Australia.*

Source: Data are from Bureau of Meteorology, Australia.

3.4.4.2 Drought in Harare, Zimbabwe

Drought is a precipitation extreme event that occurs over longer timescales, ranging from months to years. Unlike other extreme events, droughts lack a formal definition or index that is applicable globally, which makes assessments of their severity, trends in their frequency, and future projections difficult. Because of the varying indices and definitions, a qualitative assessment of drought based on precipitation is appropriate for multi-city analyses.

One city that experiences frequent and prolonged periods of drought is Harare, Zimbabwe. Over the past century, droughts have occurred several times, including 1991/1992, 1994/1995, and 1997/1998. Analysis of precipitation data reveals that precipitation in Harare has been declining over the past century at a rate of –21 mm per decade. In addition, of the ten driest July–June periods between 1938 and 2002, five have been since 1980. These results suggest that drier conditions may be becoming more frequent.

The droughts that occur in Harare have a strong connection to ENSO events. While ENSO is not the only factor that affects droughts in Zimbabwe, using this as one forecast predictor can help the city prepare and issue drought warnings with ample lead-time. However, reliance on just this predictor can be dangerous, as was the case in 1997/1998. Substantial preparations for a drought were made that year with the prediction of a strong El Niño, yet conditions did not become dry as expected (Dilley, 2000).

3.5 Future climate projections

This section describes climate change projection methods and results. The projections can be used by urban stakeholders to identify key sector-specific impacts of climate change, as a first step for developing adaptation strategies. The projection component is derived from the global climate models that focus on broad geographical scales, rather than urban climate processes. However, historical data are used for projection baselines, and these baselines reflect the effects of urban climate processes. Some of the challenges of and potential solutions to incorporating urban processes in city-specific climate projections are discussed throughout the section.

3.5.1 Global climate change projection methods

3.5.1.1 Global climate models

The theoretical impact of atmospheric greenhouse gases on the planet's energy budget has been recognized since the nineteenth century (Arrhenius, 1896). Global climate models (GCMs) are mathematical representations of climate system interactions that help quantify the impact of greenhouse gases and other system interactions. Climate models also include other climate drivers, including aerosols, land-cover changes, and solar variability. Figure 3.14 depicts physical processes that a climate model simulates.

The simulations conducted for the IPCC 2007 report were run at higher spatial resolution than prior simulations and more accurately included complex physical processes such as turbulent fluxes. Current-generation climate models capture many aspects of climate, including twentieth-century warming (when simulated using historical greenhouse gas concentrations and volcanic aerosols) (Figure 3.15). They also capture key climate characteristics of paleoclimates such as the cool Last Glacial Maximum (~21,000 years ago) and warm mid-Holocene (~6,000 years ago). Model successes over a range of historical climate conditions increase confidence that future simulations will be realistic as CO_2 concentrations continue to increase.

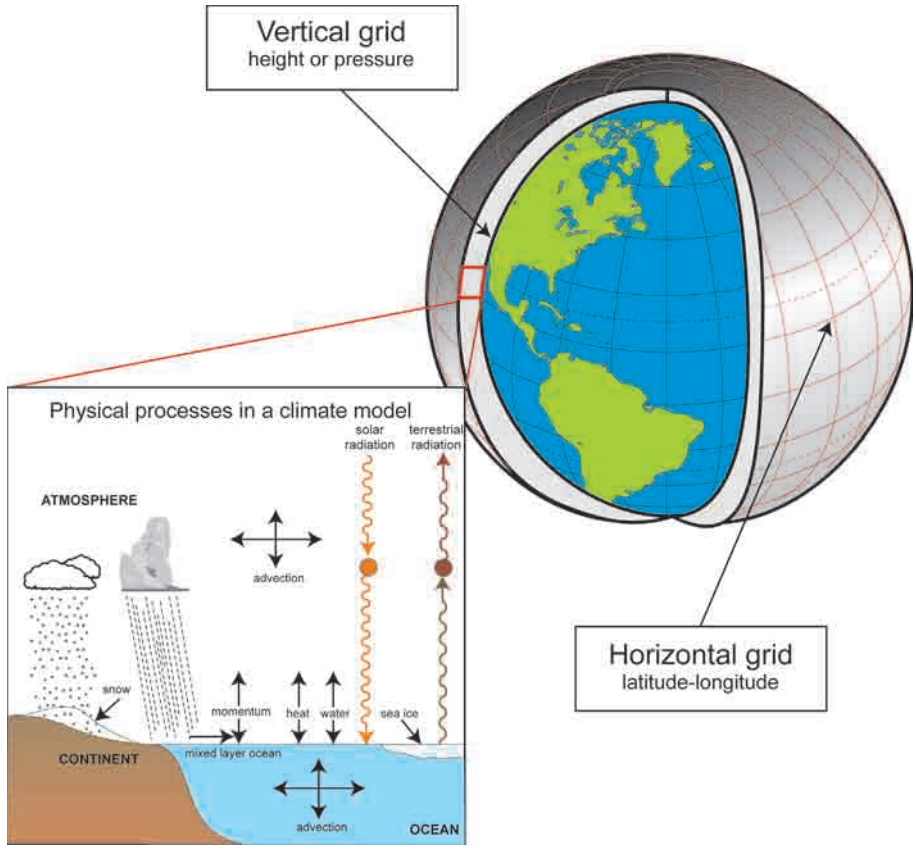

Figure 3.14: *Global Climate Model. Global climate models break the surface down into a series of gridboxes. Within each gridbox, equations are used to simulate the physical processes in the climate system.*

Source: NOAA.

3.5.1.2 Sources of uncertainty: emissions scenarios and climate sensitivity

Despite climate model advances, projections continue to be characterized by large uncertainty (for more information, see Horton *et al*., 2010). The critical uncertainties concern:

- *Future concentrations of greenhouse gases* and other climate drivers that alter the global energy balance including aerosols and black carbon;
- *Sensitivity of the climate system* to changing concentrations of climate drivers;
- *Climate variability*, which is largely unpredictable beyond one year in advance, and can mask the climate change signal at urban scales;
- *Local physical processes* such as the urban heat island, and coastal breezes that occur at smaller spatial scales than GCMs can resolve.

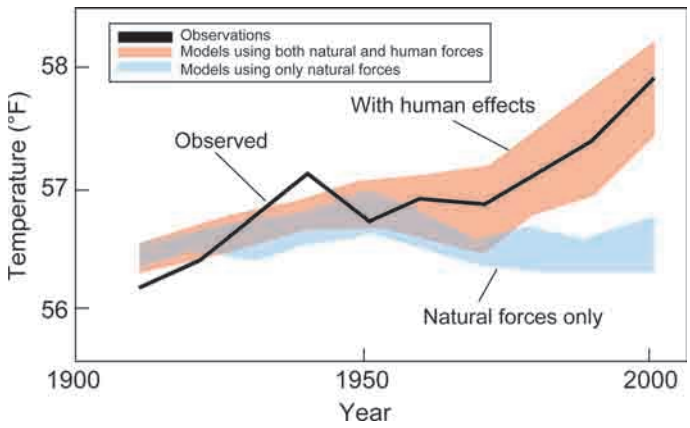

Figure 3.15: *Twentieth-century observations and GCM results. The observed temperature series follows the model simulation that includes both human effects and natural forces.*

Source: United States Global Change Research Program (2009).

These uncertainties are partially addressed here by using a suite of GCMs and greenhouse gas emissions scenarios, averaged over 30-year time periods to cancel out a portion of the unpredictable natural variability. By presenting the projections as changes through time, uncertainties associated with local physical processes are minimized, although they cannot be eliminated entirely.

3.5.1.3 Greenhouse gas emissions scenarios

Greenhouse gas emissions scenarios, described in the IPCC Special Report on Emissions Scenarios (SRES; Nakicenovic *et al*., 2000), are plausible descriptors of possible future socio-economic, technological, and governance conditions that drive energy demand and fuel choices (Parson *et al*., 2007). The greenhouse gas concentrations associated with each scenario were used as inputs for global climate model simulations. Three greenhouse

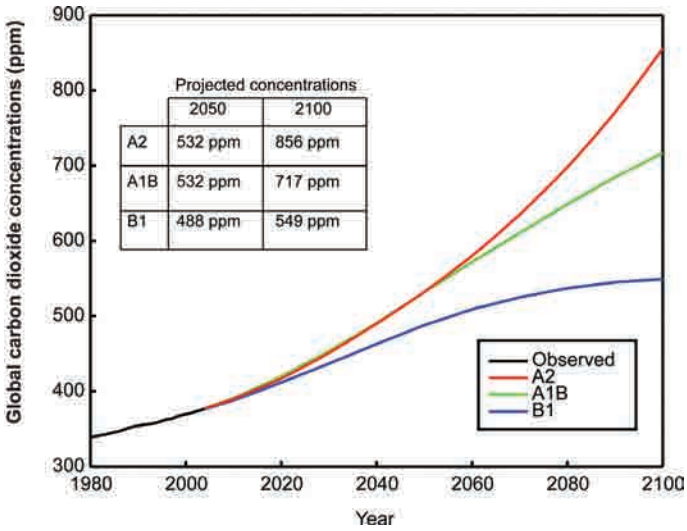

Figure 3.16: *Atmospheric CO_2 concentrations resulting from three emissions scenarios. Observed CO_2 concentrations through 2003, and future CO_2 for 2004 to 2100. The table gives the value of the CO_2 concentration for each scenario in 2050 and 2100.*

Source: IPCC (2007).

gas emissions scenarios (A2, A1B, and B1), were selected for use in this chapter. Figure 3.16 shows the CO_2 concentration associated with each of these three SRES scenarios. The three scenarios span a reasonably wide range of concentrations and allow for nominal high-, medium- and low-path CO_2 futures.

Greenhouse gas concentrations could exceed the levels in these SRES scenarios, due to increases in human emissions (for example, more rapid economic and population growth) or due to carbon and methane cycle feedbacks. As an example of the latter, increasing Arctic temperatures are leading to accelerated permafrost melting, which could lead to the release of stored methane to the atmosphere. As greenhouse gas emissions and concentrations are monitored in the coming decades, it will be possible to better assess the likelihood of high-end emissions scenarios.

3.5.1.4 Global climate model selection

From the IPCC climate model database, we selected 16 prominent models that had available output for each of the three emissions scenarios. The selected models and their space resolution are listed in Table 3.3. The outputs are collected by the World Climate Research Program (WCRP) and the Program for Climate Model Diagnosis and Intercomparison (PCMDI) (www-pcmdi.llnl.gov/ipcc/about_ ipcc.php), at the Lawrence-Livermore Laboratory in Livermore, California.

While it is unlikely that the future will closely follow a single emissions scenario, or that a GCM projection will capture all aspects of the climate system's response, using a suite of emissions scenarios and climate model simulations increases the probability that the projection range will span the actual future climate outcome. More information about the rationale for this approach, used by the IPCC, can be found in IPCC, 2007.

Table 3.3: *IPCC AR4 climate models.*

Institution	Model	Atmospheric resolution (latitude × longitude)
Bjerknes Centre for Climate Research, Norway	BCCR	2.8 × 2.8
National Weather Research Centre, METEO-FRANCE, France	CNRM	2.8 × 2.8
Canadian Center for Climate Modeling and Analysis, Canada	CCCMA	3.75 × 3.75
CSIRO Atmospheric Research, Australia	CSIRO	1.9 × 1.9
Geophysical Fluid Dynamics Laboratory, USA	GFDL1	2.0 × 2.5
Geophysical Fluid Dynamics Laboratory, USA	GFDL2	2.0 x 2.5
NASA Goddard Institute for Space Studies	GISS	4.0 × 5.0
Institute for Numerical Mathematics, Russia	INMCM	4.0 × 5.0
Pierre Simon Laplace Institute, France	IPSL	2.5 × 3.75
Frontier Research Center for Global Change, Japan	MIROC	2.8 × 2.8
Meteorological Institute of the University of Bonn, Germany	MIUB	3.75 × 3.75
Max Planck Institute for Meteorology, Germany	MPI	1.9 × 1.9
Meteorological Research Institute, Japan	MRI	2.8 × 2.8
National Center for Atmospheric Research, USA	CCSM	1.4 × 1.4
National Center for Atmospheric Research, USA	PCM	2.8 × 2.8
Hadley Centre for Climate Prediction, Met Office, UK	HadCM3	2.5 × 3.75

3.5.1.5 Model-based probability

Our combination of 16 global climate models and three emissions scenarios produces a distribution of 48 outputs for temperature and precipitation – in essence a "model-based" probability distribution. As described in Horton *et al.* (2010), future time periods are compared to a 1971–2000 model baseline. Temperature change is expressed as a difference, and precipitation as a percentage change. It should be noted that the model-based probability distribution will differ from the true probability distribution, for a range of reasons described in Horton and Rosenzweig (2010).

3.5.1.6 Downscaling

As described in Horton and Rosenzweig (2010), the projections use GCM output from a single model gridbox. Depending on the model, resolution can be as fine as ~75 – ~100 miles or as coarse as ~250 – ~275 miles. Changes from the relevant gridbox are applied to observed station data, a procedure known as the Delta Method that corrects for biases over the *baseline period* caused by factors such as the spatial mismatch between a gridbox and a point location. More sophisticated statistical and dynamical downscaling techniques can apply more localized *change projections*. While such techniques should be pursued in the future, a host of issues may hinder their utlility. These issues include: the computational cost of dynamical downscaling and the fact that statistical downscaling may be less valid as climate statistics change (Christensen *et al*., 2007).

3.5.2 Temperature, precipitation, sea level rise, and extreme events climate projections

The climate projections for temperature and precipitation for the 12 cities are presented first. For sea level rise and extreme event projections, more detailed methodologies are provided in a case study format focusing on New York City.

It is important to recognize the uncertainties associated with climate models. Therefore, the direction of change suggested here is as important as the specific numbers, which are not precise. Table 3.4 summarizes the temperature and precipitation projections for each of the cities for three future timeslices. Shown is the middle 67 percent (central range) of the model projections. Graphs showing the projections for each of the cities are shown in Figure 3.17.

3.5.2.1 Temperature

All cities are projected to see warming, with temperature increases of between 1.5 and 5.0 °C possible by the 2080s. The city expected to see the greatest warming is Toronto, Canada, with projected increase in temperature by the 2080s ranging from 2.5 to 5.0 °C.

Warming is expected to increase with distance from the equator; Toronto, for example, is expected to warm approximately two times as much as Kingston by 2100 under the A2 scenario. Warming is also generally expected to be greater in interior continental regions than in coastal regions, due to the moderating inertial influence of the oceans. This helps explain why more warming is expected in Toronto than London, even though they are at comparable latitudes. In the extra-tropical regions, warming will generally be greatest in winter.

Temperature projections for Delhi, India

Delhi, India, is one city where annual mean temperature is projected to increase over the next century. A slight upward, although not statistically significant, trend has been observed in the city from 1931 to 2005. This trend is consistent with trends from the region around Delhi in India. The region as a whole has experienced a warming trend over the past century, with the greatest warming occurring in the past three decades. The long-term warming trend appears to be driven by warmer maximum temperatures, while the more recent trend is a result of warmer maximum and minimum temperatures (Kothawale and Rupa Kumar, 2005).

Looking at Table 3.4, Delhi is projected to see an increase in annual mean temperature of between 2.5 and 4.5 °C by the

Table 3.4: *GCM projections for temperature and precipitation.*

	Temperature[a]			Precipitation[a]		
City Name	**2020s**	**2050s**	**2080s**	**2020s**	**2050s**	**2080s**
Athens	0.5 to 1.5 °C	1.0 to 4.0 °C	2.0 to 4.0 °C	–10 to +0%	–20 to –5%	–25 to –10%
Dakar	0.5 to 1.0 °C	1.0 to 2.0 °C	1.5 to 3.0 °C	–10 to +10%	–15 to +10%	–20 to +15%
Delhi	0.5 to 1.5 °C	1.5 to 2.5 °C	2.5 to 4.5 °C	–10 to +20%	–15 to +35%	–15 to +35%
Harare	0.5 to 1.5 °C	1.5 to 2.5 °C	2.0 to 4.0 °C	–10 to +5%	–10 to +5%	–15 to +5%
Kingston	0.5 to 1.0 °C	1.0 to 1.5 °C	1.5 to 2.5 °C	–10 to +5%	–25 to +0%	–30 to –5%
London	0.5 to 1.0 °C	1.0 to 2.0 °C	1.5 to 3.0 °C	–5 to +5%	–5 to +5%	–5 to +5%
Melbourne	0.5 to 1.0 °C	1.0 to 2.0 °C	1.5 to 3.0 °C	–10 to +5%	–15 to +0%	–20 to +0%
New York	1.0 to 1.5 °C	1.5 to 3.0 °C	2.0 to 4.0 °C	+0 to +5 %	+0 to +10%	+5 to +10%
Sao Paulo	0.5 to 1.0 °C	1.0 to 2.0 °C	1.5 to 3.5 °C	–5 to +5%	–5 to +5%	–10 to +5%
Shanghai	0.5 to 1.0 °C	1.5 to 2.5 °C	2.0 to 4.0 °C	–5 to +5%	+0 to +10%	+0 to +15%
Tokyo	0.5 to 1.0 °C	1.5 to 2.5 °C	2.0 to 4.0 °C	–5 to +5%	+0 to +5%	+0 to +10%
Toronto	1.0 to 1.5 °C	2.0 to 3.0 °C	2.5 to 5.0 °C	+0 to +5%	+0 to +10%	+0 to +15%

Shown is the central range (middle 67 percent) of values from model-based probabilities; temperatures ranges are rounded to the nearest half-degree and precipitation to the nearest 5 percent.

[a] Based on 16 GCMs and three emissions scenarios.

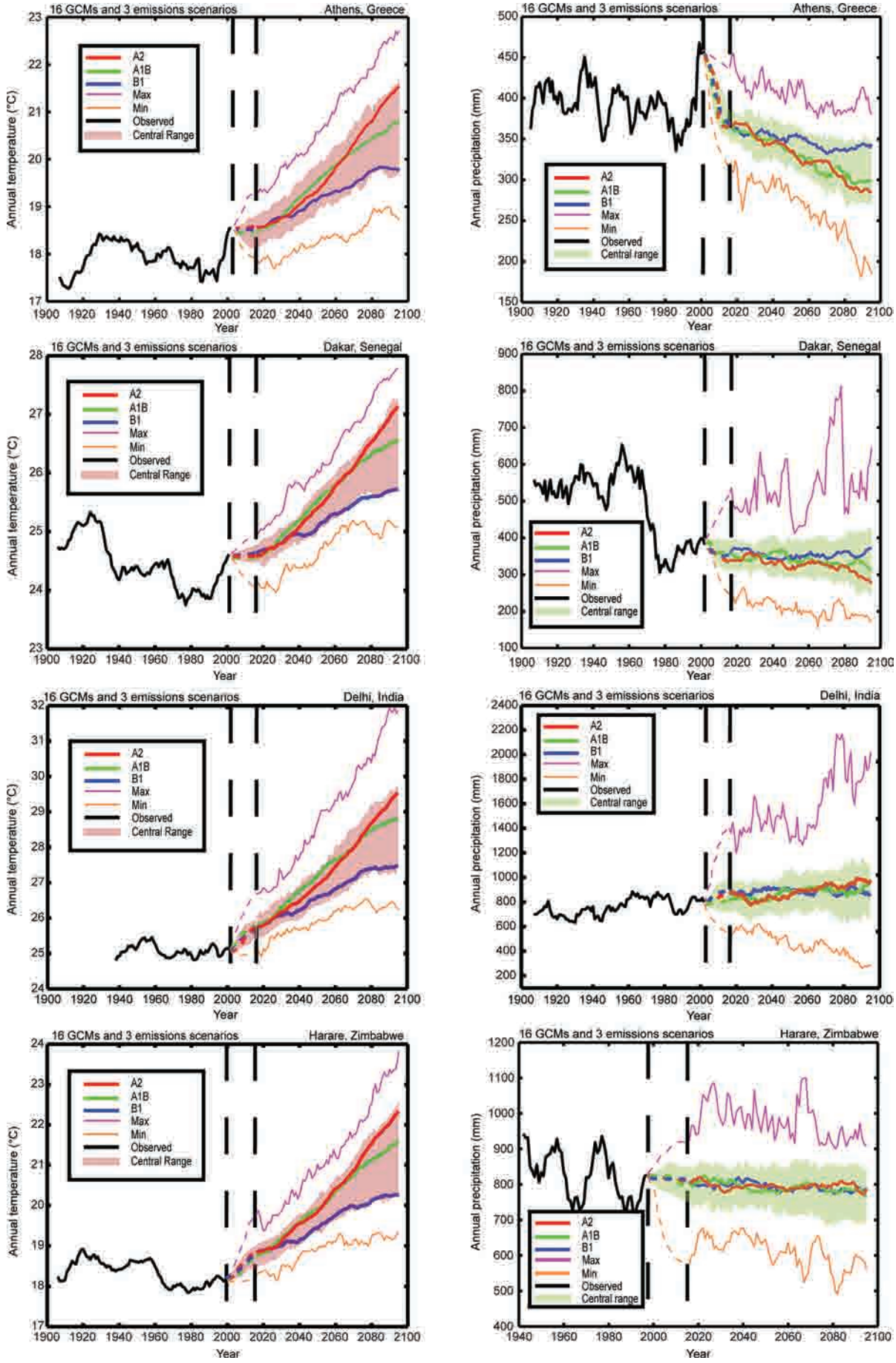

Figure 3.17: *Observed and projected temperature and precipitation. Combined observed (black line) and projected temperature and precipitation is shown. Projected model changes through time are applied to the observed historical data. The three thick lines (green, red, and blue) show the average for each emissions scenario across the 16 GCMs. Shading shows the central range. The bottom and top lines, respectively, show each year's minimum and maximum projections across the suite of simulations. A 10-year filter has been applied to the observed data and model output. The dotted area between represents the period that is not covered due to the smoothing procedure. WCRP, PCMDI, and observed data sources found in Table 3. 2. Note differences in temperature and precipitation scales.*

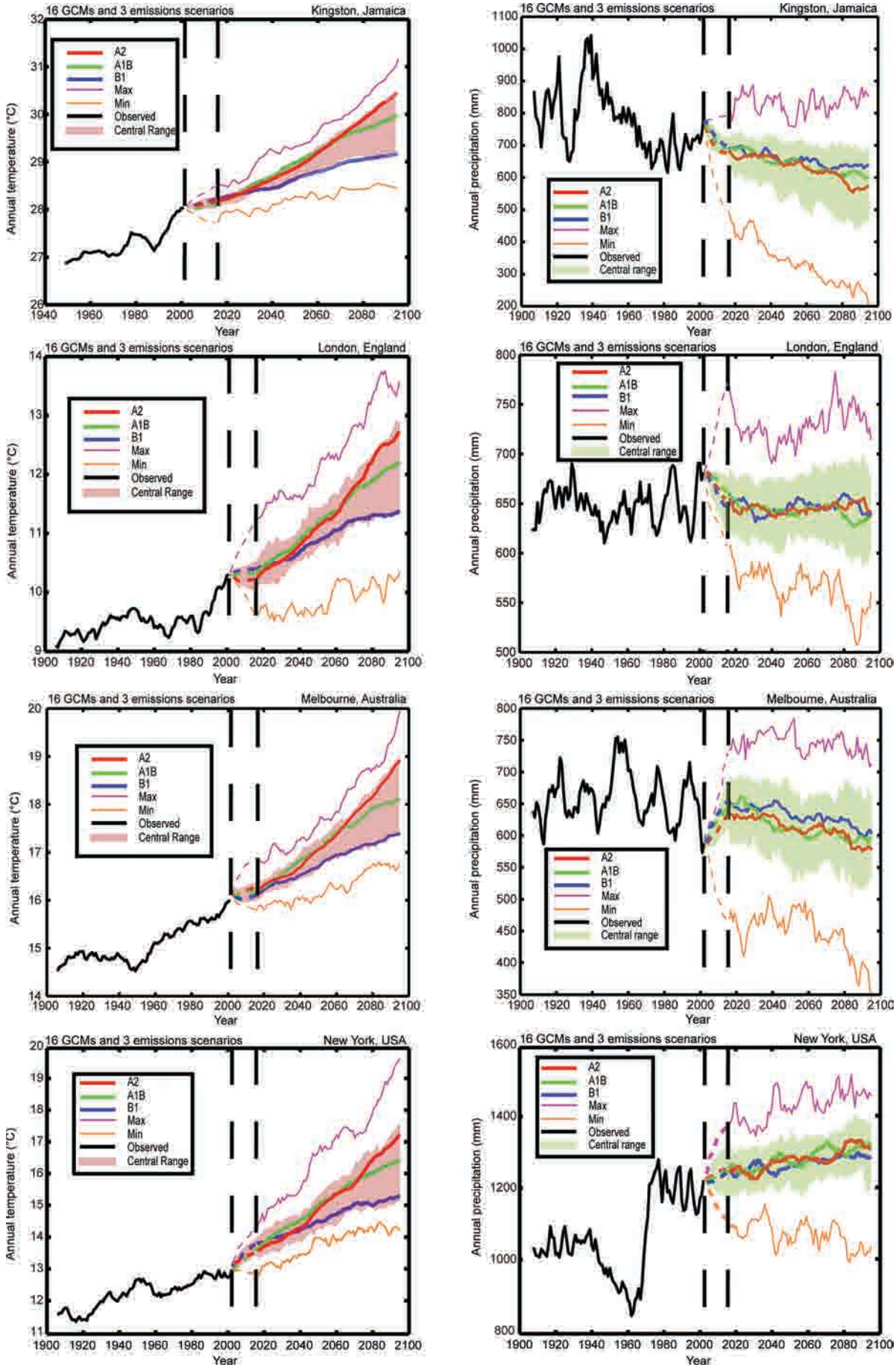

Figure 3.17: *(continued)*

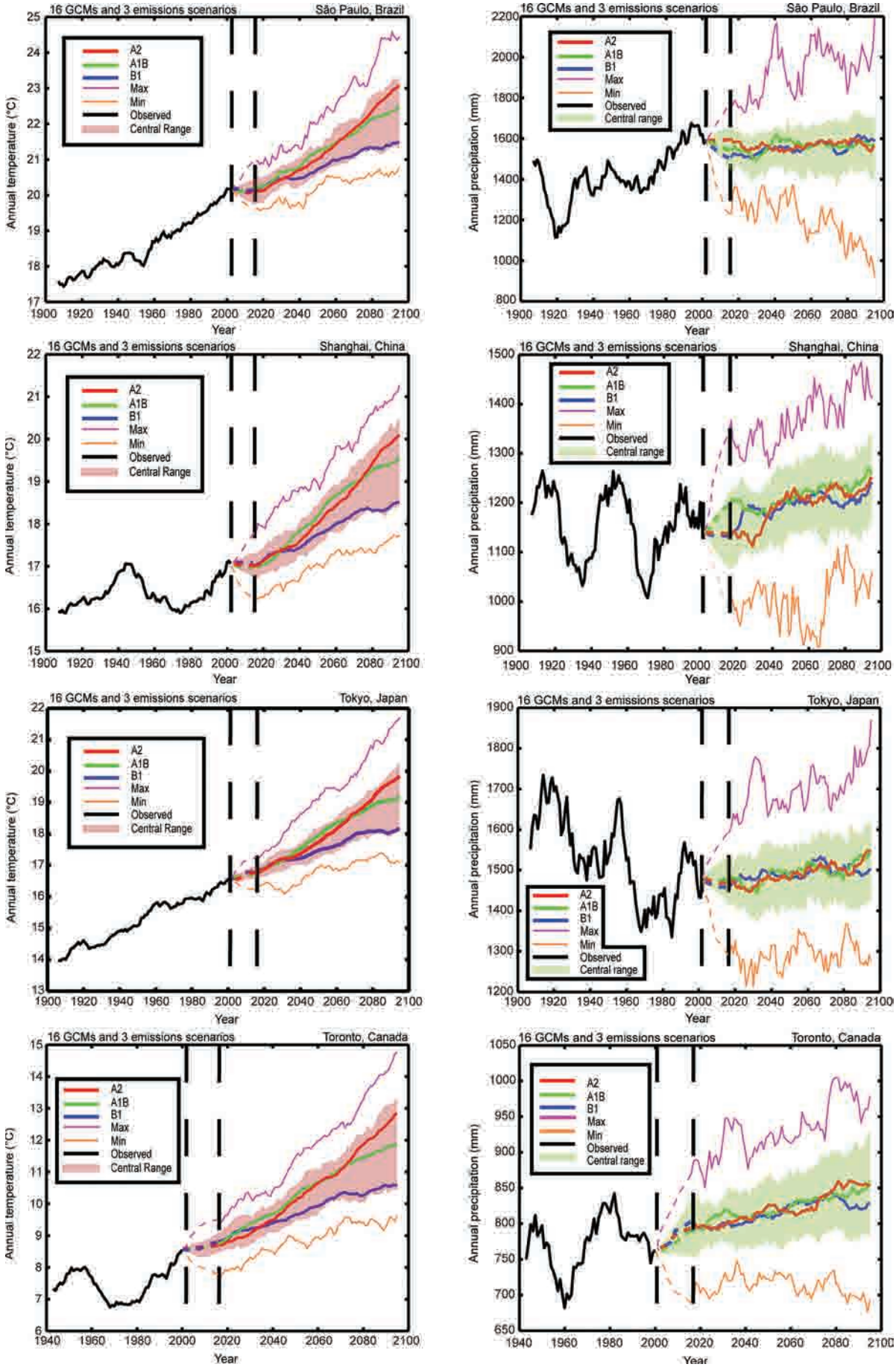

Figure 3.17: *(continued)*

2080s. Figure 3.17 shows the full range of GCM projections for annual mean temperature for Delhi. Only around the 2030s do differences between the emissions scenarios emerge.

3.5.2.2 Precipitation

There is greater variability in the direction of projections of percentage change in precipitation for these cities. Some cities are expected to see increases in precipitation while others are projected to experience sharp declines in precipitation by the 2080s. For cities in higher latitudes projected to see increased precipitation, such as Toronto and New York, most of the precipitation increase will be in the form of rainfall, as snowfall is likely to decline given the warmer temperatures.

Precipitation changes will differ dramatically by region. In general, mid-to-high latitude cities such as Toronto, New York, and Tokyo are expected to experience precipitation increases. However, some mid-latitude cities, such as London, are expected to experience significant summer-time drying, which could lead to net precipitation decreases. Other cities at the boundaries between the mid-latitudes and subtropics are expected to experience drying, including Harare and Melbourne. Some tropical cities are expected to experience more precipitation, while others are expected to experience less. In those cities where precipitation is strongly correlated with inter-annual variability, changes in the modes with climate change will be critical, and introduce an added element of uncertainty. These cities include Harare, Melbourne, Delhi, and São Paulo for ENSO, and Athens and London for the NAO.

It is important to note that in some cases the GCMs have trouble accurately simulating the baseline/observed precipitation in particular regions. This is especially true in cities that have strong seasonal precipitation cycles. With a poor handle on the baseline, the projections for the city are therefore skewed. The projections for Delhi, which has a monsoonal climate, provide an example of this, as extreme values for increased precipitation may overestimate how wet the climate may become. It is therefore important to focus on the direction of change, not so much the actual values. Because it was not possible to include all cities across the globe, the projections presented here can be used as a proxy for other cities with similar climate conditions.

Precipitation projections for Athens, Greece

Athens is one city where annual precipitation is projected to decrease over the next century. In the observed climate record for annual precipitation, there is no statistically significant trend. Slight decreasing trends in other precipitation variables, such as wet days, have been observed. What appears to be occurring in Greece, as well as many other parts of the globe, is an increase in extreme daily precipitation (Nastos and Zerefos, 2007). While total rainfall and the number of wet days show no change or a decline, when there is precipitation, it is more intense. This could potentially be most damaging, as these rain events can cause short-duration, flash flooding.

As shown in Table 3.4 Athens is projected to see drops in precipitation between 10 and 25 percent by the 2080s. Although seasonal projections are less certain than annual results, the climate models project much of the drying to occur during the summer months. Figure 3.17 shows the full range of GCM projections for annual total precipitation in Athens. Even using 10-year smoothing, there remains large historical variability in the observed trend. For the projections, only from approximately the 2040s onward does the B1 scenario produce smaller precipitation decreases compared to the other two scenarios.

3.5.2.3 Sea level rise

As the oceans warm and expand and land-based ice continues to melt, all the coastal cities analyzed here are expected to experience sea level rise this century. However, the rate will differ by city, for two primary reasons. First, the local height of the adjacent ocean can differ by city, due to the influence of ocean currents, water temperature, and salinity, and the influence of wind and air pressure. Second, local land height change can differ by city. Some cities such as Shanghai are sinking due to the effects of groundwater extraction and compaction of soils by the expanding built environment.

Projections for sea level rise are presented in a case study format for New York City. Described are the methods used to make these projections and the projections themselves. Most of the text in this section is from Horton and Rosenzweig (2010).

Sea level rise methods

The GCM-based methods used to project sea level rise for the New York City region include both global (global thermal expansion and meltwater from glaciers, ice caps, and ice sheets) and local (local land subsidence and local water surface elevation) components.

Within the scientific community, there has been extensive discussion of the possibility that the GCM approach to sea level rise may underestimate the range of possible increases, in large part because it does not fully consider the potential for land-based ice sheets to melt due to dynamical (motion-related) processes (Horton *et al.*, 2008). For this reason, the NPCC developed an alternative "rapid ice-melt" approach for regional sea level rise projection based on observed trends in melting of the West Antarctic (Velicogna and Wahr, 2006) and Greenland ice sheets (Rignot and Kanagaratnam, 2006) and paleoclimate studies of ice-melt rates during the most recent postglacial period (Fairbanks, 1989). Starting around 20,000 years ago, global sea level rose 120 meters and reached nearly present-day levels around 8,000–7,000 years ago. The average rate of sea level rise during this ~10,000–12,000 year period was 9.9 to 11.9 cm per decade. This information is incorporated into the rapid ice-melt scenario projections.

The GCM-based sea level rise projections indicate that sea level in New York City may rise by 5 to 13 centimeters in the

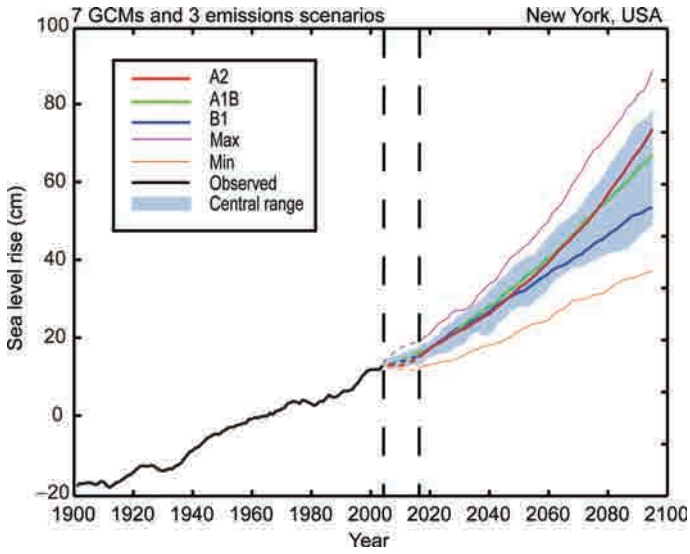

Figure 3.18: *New York City sea level rise. Combined observed (black line) and projected sea level rise is shown. Projected model changes through time are applied to the observed historical data. The three thick lines (green, red, and blue) show the average for each emissions scenario across the seven GCMs used for sea level rise. Shading shows the central range. The bottom and top lines, respectively, show each year's minimum and maximum projections across the suite of simulations. A 10-year filter has been applied to the observed data and model output. The dotted area between 2002 and 2015 represents the period that is not covered due to the smoothing procedure.*

Source: WCRP, PCMDI, and observed data from NOAA Tides and Currents.

2020s, 18 to 30 centimeters in the 2050s, and 30 to 58 centimeters in the 2080s. Sea level projections for the three emissions scenarios agree through the 2040s. Figure 3.18 shows that the B1 scenario produces smaller increases in sea level than the A1B and A2 scenarios beginning in the 2050s, and only around 2080 does the A2 scenario produce larger values than A1B. The divergence of A2 from A1B occurs approximately 10 years earlier for temperature than for sea level rise, in part reflecting the large inertia of the ocean and ice sheets relative to the atmosphere.

Sea level rise projections for the New York City region are higher than global sea level rise projections (generally by approximately 15 cm for twenty-first century projections) (IPCC, 2007). One reason is that the New York metropolitan region is subsiding by approximately 8 to 10 cm per century. The climate models also have a tendency to produce accelerated sea level rise along the northeast US coast, associated in large part with a projected weakening of the Gulf Stream (Yin *et al.*, 2009).

The model-based sea level rise projections shown in Table 3.5 are characterized by greater uncertainty than the temperature projections, due largely to the possibility that dynamic processes in polar ice sheets not captured by the GCMs may accelerate melting beyond currently projected levels. This uncertainty is weighted towards the upper bound: that is, the probability of sea level rise lower than that described in the GCM-based projections in Table 3.5 is very low, and the probability of sea level rise exceeding the GCM projections is relatively high.

Table 3.5: *Sea level rise projections including the rapid ice-melt scenario for New York City.*

New York City	2020s	2050s	2080s
Sea level rise[a]	+5 to 13 cm	+18 to 30 cm	+30 to 58 cm
Rapid ice-melt sea level rise[b]	~13 to 25 cm	~48 to 74 cm	~104 to 140 cm

[a] Based on seven GCMs and three emissions scenarios.

[b] "Rapid ice-melt scenario" is based on acceleration of recent rates of ice-melt in the Greenland and West Antarctic ice sheets and paleoclimate studies.

The rapid ice-melt sea level rise scenario addresses this possibility. It is based on extrapolation of recent accelerating rates of ice-melt from the Greenland and West Antarctic ice sheets and on paleoclimate studies that suggest sea level rise on the order of 9.9 to 11.9 cm per decade may be possible. Sea level rise projections for New York City in the rapid ice-melt scenario are shown in the bottom row of Table 3.5. The potential for rapid ice-melt is included in the regional projections for New York City because of the great socio-economic consequences should it occur. To assess the risk of accelerated sea level rise and climate change for the New York City region over the coming years, climate experts need to monitor rates of polar ice-melt, as well as other key indicators of global and regional climate change.

3.5.2.4 Extreme events

Some of the largest climate change effects on cities are associated with extreme events, such as heat waves, intense precipitation events, and coastal storms. The frequency, intensity, and duration of many extreme events are expected to increase with climate change. The following quantitative New York City example describes the types of extreme event threats faced by many cities, although each city will face slightly different extreme event and natural disaster risks.

Following the New York City case, we present an example of qualitative projections for tropical cyclones, an extreme event that impacts many cities included in this chapter. It should be noted that extreme climate events and natural disasters are intertwined, partly because climate hazards represent a major portion of all natural disasters. Furthermore, climate extremes (such as intense precipitation or drought-induced forest fires) may cause secondary natural disasters (such as landslides). The following section is a case of extreme event projections for New York City, from Horton and Rosenzweig, (2010) and Horton *et al.*, (2010).

Extreme events projections for New York City

Extremes of temperature and precipitation (with the exception of drought) tend to have their largest impacts at daily rather than monthly timescales. Because monthly output from climate models is considered more reliable than daily output, simulated changes in monthly temperature and precipitation were calculated; monthly changes through time from each of the 16 GCMs and three emissions scenarios described earlier in this section

[ADAPTATION] Box 3.3 Adaptation to sea level rise in Wellington, New Zealand

Chris Cameron, Paul Kos and Nenad Petrovic

Wellington City Council

INTRODUCTION

Wellington is a coastal city, with an inner harbor and exposed southern coast. A pilot study focusing on the impacts of sea level rise on a low-lying city suburb has commenced to inform the adaptation approach across the city.

Part of the area included in this pilot study (Box Figure 3.3) has been identified as a key growth node for urban intensification. The area also contains a range of key infrastructure including a significant highway, an international airport, utilities, businesses, housing, and community facilities such as schools, pools, libraries, a marina, and a surfing beach.

METHODOLOGY

Sea level rise was viewed as one of the most critical climate change impacts on the study area, because it lies between only 1 m and 3 m elevation.

Box Figure 3.3: *The study area.*

The latest New Zealand guidance on coastal hazards[2] associated with climate change recommends that councils consider the impacts of a 0.8 m increase in sea level by 2090. However, given the considerable uncertainty in projections and the possibility of catastrophic events, an approach was taken based on testing infrastructure resilience and response via a range of scenarios. This will allow the development of strategies to manage the expected risk.

Three core scenarios were examined (0.5 m, 1 m, and 2 m) with each having an additional 0.5 m storm surge component within the harbour and a 1 m component on the exposed southern coast. These scenarios reflect the most recent scientific probabilities in the short term (50–100 years), while allowing for possible higher levels in the longer term.

Evaluation of the scenarios was carried out in an interdisciplinary cross-council workshop including water, drainage, roading, hazards, transport, coastal and recreational, and urban planning experts. For each asset the following information was gathered: description, ownership, criticality, condition, relocatability, economic value, proposed upgrades. Each asset was then tested against each sea level rise scenario to determine potential risks and impacts. Feasible response options were then proposed.

Mapping the scenarios

Sea level rise scenarios were mapped based on ground elevation data from LiDAR (Light Detection And Ranging). The LiDAR data were captured at 1 cm vertical intervals with +/–10 cm accuracy and were verified by field survey. The data were then used to create a digital terrain model. A local vertical datum was developed based on mean high water springs. This allowed for assessment of the highest likely sea level that includes mean tidal elements.

Infrastructure and key existing community facilities were mapped against the sea level rise scenarios so the impacts could be evaluated holistically.

RESULTS

Through qualitative assessment of likely impacts and appropriate responses to the sea level rise scenarios a number of issues were identified:

- Degradation of the level of service from the storm-water system
- Rising groundwater levels
- Need to evaluate response options for at-risk coastal areas across the city
- Need for early decision-making for response planning
- Interactions and interdependency between assets
- Need to prioritise adaptation responses across the city

The workshop highlighted that rising sea levels are likely to have some impacts on the storm-water system in the short

2 See www.mfe.govt.nz/publications/climate/preparing-for-coastal-change-guide-for-local-govt/index.html.

term (next 20–30 years). Some solutions were proffered that could be developed as part of normal asset management.

Low-lying parts of the study area may be susceptible to increased flooding due to a rise in the water-table. This was regarded as more urgent than "over-topping." Several likely options for responding were identified and will be consulted on with Councillors and the community. Further detailed work is required to examine the impact, behavior, and response of groundwater in the study area, together with the likely costs and benefits of each response option.

Different responses may be appropriate for the natural dune environment of the southern coast compared to the structurally modified northern coast. Maintaining a dune environment on the south coast would help the area retain its high aesthetic and amenity values. Moreover, this could be a more successful adaptation response, given the adverse effects that "hard engineered" structures can have on a beach.

The importance of taking into consideration linkages between infrastructure elements was recognised. For example, pumping stations require power and telecommunications, which must therefore be maintained through the area at all times.

Similar impacts may occur in other parts of the city, and an overall cost–benefit analysis cannot be completed in isolation within a limited area.

These findings will inform the proposed intensification plans and other ongoing development, maintenance, and asset management plans for the area. Findings will also be used for discussions within council and the community around prioritizing, costs, and residual risks.

CONCLUSIONS

This study gathered and evaluated key information needed to make an initial assessment of climate change impacts in a localized urban area. It has indicated where further detailed work could be undertaken to derive a more accurate assessment of costs and benefits. A modified approach based on this pilot study will be used across other coastal areas within Wellington City.

[ADAPTATION] Box 3.4 Climate change adaptation in Kokkola, Finland

Philipp Schmidt-Thomé

Geological Survey of Finland

Juhani Hannila

Technical Service Centre, City of Kokkola

Kokkola, a medium-sized town on the west coast of Finland, was one case study of the Developing Policies & Adaptation Strategies to Climate Change in the Baltic Sea Region (ASTRA) project. The award-winning ASTRA project was co-financed by the European Regional Development Fund (ERDF) under the INTERREG IIIB Programme. The ASTRA (www.astra-project.org) and SEAREG (www.gtk.fi/dsf) projects are the predecessors of the currently ongoing BaltCICA project (www.baltcica.org). The aim of the projects is to support planners and decision-makers in understanding the potential impacts of climate change on regional development and to support the implementation of adaptation strategies. While SEAREG (2002–2005) mainly focused on awareness raising, ASTRA (2005–2007) went a step further to support the development of adaptation strategies. BaltCICA (2009–2012) builds on the results of the projects by implementing adaptation measures in cooperation with stakeholders. All three projects are managed by the Geological Survey of Finland (GTK) and count on partners from the Baltic Sea Region.

Kokkola was founded in 1620 adjacent to the Bothnian Bay (Baltic Sea). The postglacial rebound (land uplift) in this area amounts to 9 mm per year, and due to the retreating sea the original city center now lies about 2 km inland from the shoreline. Rising sea levels have made the glacial rebound less effective over recent years so that the net land rise has dropped to about 4–5 mm per year relative to the mean sea level. Normal sea level variation in Kokkola is between –1.0 m and +1.5 m relative to mean sea level. The city planning office of Kokkola was thus interested in sea level rise scenarios for the twenty-first century. The background is that Kokkola experiences a strong pressure for coastal housing development. If the coastal land uplift continued as at present, the coastal areas could be easily developed, even with the lower glacial rebound effect of 5 mm per year. But what if the sea level rise and storm flood events become stronger and flood patterns change?

Kokkola participated in the ASTRA project to better understand the climate change scenarios and to evaluate how these can be implemented into local planning. The uncertainties of the climate change scenarios especially played an important role in the assessments. Finally the city chose to use the MPIA2 "high case" sea level change scenario originally developed under the SEAREG project. According to these scenarios it is possible that the land uplift will be neutralized by sea level rise; in other words, the present coastline would not change over the twenty-first century. Consequently, the often predicted increasing wind speed peaks during storm events and the increase in heavy rainfalls would lead to flood-prone area changes. Two important locations for future housing development in Kokkola are the area of the 2011 housing fair and Bride Island.

The area for the housing fair, to be held in 2011, was planned several years ago. Such a housing fair is an important event in Finland, as the houses built for the fair are later to be used

for housing, which is an important asset for the investors. The housing fair in Kokkola is planned in a new housing area on the sea shore. In the course of the ASTRA project the location of the housing fair 2011 was not changed, but the minimum elevation of the building ground above mean sea level was raised by 1.0–1.2 m compared to previous plans on the sea shore and is about 3.5 m (streets 3.0 m) above the mean sea level. In other words, the decision was taken that sea shore plots may be built up, but it has to be made sure that the lowest floor of the houses is well above potential flood levels. The cost of each plot and house was calculated, including the artificial elevation of the building ground, and the investors were willing to accept this extra cost because the demand for houses located on the sea shore is still rising.

The second example, Bride Island, is a very popular place for summer cottages in the close vicinity of the city. The current trend in many European countries is to improve these temporary summer homes into cottages that can be used all year round, and even to convert them into permanent homes. If the land were to continue to rise out of the sea as it has done so far, such a conversion from a temporary to a permanent home would pose no problem. The interest of the land owners is not only in converting the houses; the investments certainly would also be justified by rising land and house prices. The city of Kokkola, on the other hand, carries responsibilities if land use plans are changed and natural hazards start to threaten housing areas. Due to the scenarios used in the ASTRA project, land use plan changes for Bride Island were put on hold until improved climate change scenarios and observed trends have been analyzed. However, sea level change scenarios are taken into account in the minimum elevation of buildings above mean sea level, e.g., when old cottages are renovated. Lowest building elevation for the newest building permits has been raised to 2.5 m above the mean sea level – so, in building renovation the adaptation to sea level rise is put into practice in small steps or plot by plot.

Recommendations of the ASTRA report were also taken into account in building and city planning regulations. Several regulations are in place to protect from rising wind speeds, cold winds, and storms on the shore. For example, low houses with optimal roof pitch against wind turbulence on yards; inner courtyards towards the south; plantations and fencing against cold wind directions; and also directing main streets crosswise to the coldest winds to avoid wind tunnel effects.

The city of Kokkola is not taking part in the ASTRA follow-up project BaltCICA because, for now, all important decisions on climate change adaptation have been taken or are under discussion. Nevertheless, the city stays in close contact with the Geological Survey of Finland in order to be informed in a timely manner about the latest research results.

were then applied to the observed daily Central Park record from 1971 to 2000 to generate 48 time series of daily data.[3] This is a simplified approach to projections of extreme events, since it does not allow for possible changes in the patterns of climate variability through time. However, because changes in variability for most climate hazards are considered highly uncertain, the approach described provides an initial evaluation of how extreme events may change in the future. This level of information with appropriate caveats can assist long-term planners as they begin to prepare adaptation strategies to cope with future extreme events.

Despite their brief duration, extreme events can have large impacts on cities, so they are a critical component of climate change impact assessment. Table 3.6 indicates how the frequency of heat waves, cold events, intense precipitation, drought, and coastal flooding in the New York City region are projected to change in the coming decades. The average number of extreme events per year for the baseline period is shown, along with the central 67 percent of the range of the model-based projections.

The total number of hot days, defined as days with a maximum temperature over 32 or 38 °C, is expected to increase as the twenty-first century progresses. The frequency and duration of heat waves, defined as three or more consecutive days with maximum temperatures above 32 °C, are also expected to increase. In contrast, extreme cold events, defined as the number of days per year with minimum temperature below 0 °C, are expected to become rarer.

Although the percentage increase in annual precipitation is expected to be relatively small in New York, larger percentage increases are expected in the frequency, intensity, and duration of extreme precipitation (defined as more than 25 mm, 50 mm, and 100 mm per day). This projection is consistent both with theory – a warmer atmosphere is expected to hold more moisture, and while evaporation is a gradual process, precipitation tends to be concentrated in extreme events – and observed trends nationally over the twentieth century (Karl and Knight, 1998).

Due to higher projected temperatures, twenty-first century drought projections reflect the competing influences of more total precipitation and more evaporation. By the end of the twenty-first century the effect of higher temperatures, especially during the warm months, on evaporation is expected to outweigh the increase in precipitation, leading to more droughts, although the timing and levels of drought projections are marked by relatively large uncertainty. The rapid increase in drought risk through time is reflective of a non-linear response, because as temperature increases in summer become large, potential evaporation increases dramatically. Because the New York Metropolitan Region has experienced severe multi-year

3 Because they are rare, the drought and coastal storm projections were based on longer time periods.

Table 3.6: *Quantitative changes in extreme events.*

	Extreme event	*Baseline (1971–2000)*	2020s	2050s	2080s
Heat waves and cold events	Number of days/year with maximum temperature exceeding:				
	~32 °C	*14*	23 to 29	29 to 45	37 to 64
	~38 °C	*0.4*[a]	0.6 to 1	1 to 4	2 to 9
	Number of heat waves/year[b]	*2*	3 to 4	4 to 6	5 to 8
	Average duration (in days)	*4*	4 to 5	5	5 to 7
	Number of days/year with minimum temperature at or below 0 °C	*72*	53 to 61	45 to 54	36 to 49
Intense precipitation and droughts	Number of days per year with rainfall exceeding ~25 mm	*13*	13 to 14	13 to 15	14 to 16
	Drought to occur, on average[c]	*~once every 100 years*	~once every 100 years	~once every 50 to 100 years	~once every 8 to 100 years
Coastal floods and storms[d]	1-in-10 year flood to reoccur, on average	*~once every 10 years*	~once every 8 to 10 years	~once every 3 to 6 years	~once every 1 to 3 years
	Flood heights (m) associated with 1-in-10 year flood	*1.9*	2.0 to 2.1	2.1 to 2.2	2.3 to 2.5
	1-in-100 year flood to reoccur, on average	*~once every 100 years*	~once every 65 to 80 years	~once every 35 to 55 years	~once every 15 to 35 years
	Flood heights (m) associated with 1-in-100 year flood	*2.6*	2.7 to 2.8	2.8 to 2.9	2.9 to 3.2

The central range (middle 67 percent of values from model-based probabilities) across the GCMs and greenhouse gas emissions scenarios is shown.

[a] Decimal places shown for values less than 1 (and for all flood heights).

[b] Defined as three or more consecutive days with maximum temperature exceeding ~32 °C.

[c] Based on minima of the Palmer Drought Severity Index (PDSI) over any 12 consecutive months.

[d] Does not include the rapid ice-melt scenario.

droughts during the twentieth century – most notably the 1960s "drought of record" – any increase in drought frequency, intensity, or duration could have serious implications for water resources in the region. Changes in the distribution of precipitation throughout the year, and timing of snow-melt, could potentially make drought more frequent as well. According to the IPCC, snow season length is very likely to decrease over North America (IPCC, 2007).

As sea level rises, coastal flooding associated with storms will very likely increase in intensity, frequency, and duration. The changes in coastal floods shown here are solely due to the IPCC model-based projections of gradual changes in sea level through time. Any increase in the frequency or intensity of storms themselves would result in even more frequent future flood occurrences. By the end of the twenty-first century, projections based on sea level rise alone suggest that coastal flood levels that currently occur on average once per decade may occur once every one-to-three years (see Table 3.6).

The projections for flooding associated with more severe storms (e.g., the 1-in-100 year storm) are less well characterized than those for less severe storms (e.g., the 1-in-10 year events), for multiple reasons. The historical record is not sufficiently long to allow precise estimates of the flood level associated with the once per century storm. Furthermore, the storm risk may vary on multi-decadal to centennial ocean circulation-driven timescales that are currently not well understood. Keeping these uncertainties in mind, we estimate that, due to sea level rise alone, the 1-in-100 year flood may occur approximately four times as often by the 2080s.

Tropical cyclones

One extreme climate event that impacts many cities around the globe is tropical cyclones. Of the cities used in the chapter, several are at risk of being impacted by these storms, which bring heavy rainfall, high winds, and coastal storm surge. Kingston is one city at risk of tropical cyclones and, in recent years, several storms have affected the island of Jamaica. These storms

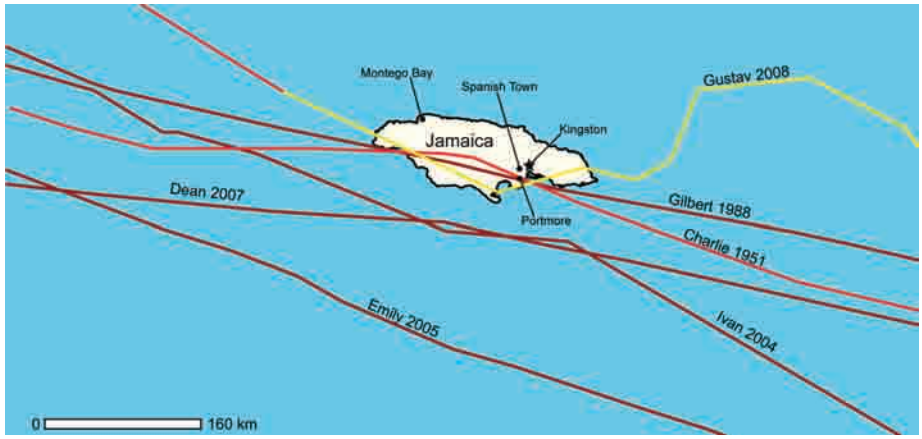

Figure 3.19: *Hurricane tracks near Kingston, Jamaica.*

Source: Adapted from NOAA.

include Ivan (2004), Emily (2005), Dean (2007), and Gustav (2008). Figure 3.19 shows the tracks of these storms along with two others, Charlie (1951) and Gilbert (1988).

Perhaps the most devastating storm to hit the island was Hurricane Gilbert in 1988, which had winds over 50 m/s as it passed over the island. Heavy rainfall and a storm surge close to 3 m caused 45 deaths and over US$2 billion in damage (Lawrence and Gross, 1989).

There is much uncertainty as to how the frequency and strength of tropical cyclones will change with global climate change. Patterns of natural climate variability, including El Niño–Southern Oscillation (ENSO) and Atlantic Multidecadal

[VULNERABILITY] Box 3.5 Lessons from a major climate event: Hurricane Katrina and New Orleans

Alexander S. Kolker

Louisiana Universities Marine Consortium, Chauvin, LA

Douglas J. Meffert

Center for Bioenvironmental Research, Tulane and Xavier Universities, New Orleans LA

Armando Carbonell

Department of Planning and Urban Form, Lincoln Institute of Land Policy, Cambridge, MA

Stephen A. Nelson

Department of Earth and Environmental Sciences, Tulane University, New Orleans, LA

Few cities in developed countries have felt the impacts of climatic processes as has New Orleans. On the morning of August 29, 2005, Hurricane Katrina made landfall in south Louisiana and again in Mississippi. It produced storm surges that ruptured levees on drainage and navigation canals that catastrophically flooded the City of New Orleans. Rapidly rising waters were met by an inadequate governmental response. In the process, well over 1400 people died, and many more lives were forever changed.

Katrina was a massive storm, fueled by very warm waters in the Gulf of Mexico; however, uncertainty exists as to whether Katrina's strength was exacerbated by climate change. The northern Gulf of Mexico is historically hurricane prone, and has experienced large storms throughout the past 3000 years (Liu and Fearn, 2000). The power of Atlantic hurricanes appears to have increased over the past three decades (Emanuel, 2005), though this view is not accepted by all experts (Trenberth and Fasullo, 2008). However, climate models generally predict that global warming will increase the severity and/or intensity of tropical cyclones (IPCC, 2007), and Hurricane Katrina provides important lessons into how cities choose to adapt to and mitigate future climate change.

One lesson is that a city's physical landscape strongly affects its response to climate events. New Orleans developed along a series of natural levees at the banks of the Mississippi River and its former distributaries and the city's geography can be traced to alluvial processes. Rivers deposit their largest and heaviest particles closest to the main channel, and these natural levees were the high stable grounds where the city was originally settled (Coleman *et al*., 1998; Coleman and Prior, 1980; Gould, 1970). As the city expanded in the late 19th and 20th centuries, lower-lying areas comprised of muddy, organic-rich sediments were developed. These areas were drained, and once dried out, subsided rapidly (Rogers et al., 2008; Nelson and LeClair, 2006; Kolb and Saucier, 1992). In the present city of New Orleans elevation, subsidence rates and depth of flooding following Katrina are roughly proportional to age, with younger regions typically being the lower, wetter, and more rapidly subsiding (Dixon *et al*., 2006; Seed *et al*., 2008; Russell, 2005).

New Orleans's geology also has important implications for the stability of the city's levees and its vulnerability to sea level rise. High subsidence rates in the delta plain contributed to one of the highest rates of relative sea level rise on Earth (Tornqvist *et al*., 2008, Reed, 2002; Day *et al*., 2007), which makes New Orleans a data-rich model for examining how cities respond to climatically driven sea-level rise. Subsidence lowered elevation of many of the city's levees while and peat and sand bodies below them allowed for subsurface water flow that undermined their stability (Rogers *et al*., 2008, Seed *et al*., 2008). Levee instability was also caused by engineering failures that are discussed below. Human activities have exacerbated wetland loss in the Mississippi Delta plain, at rates that now stand near 50 km^2 yr^{-1} (Day *et al*., 2007; Barras *et al*., 2003; Morton, Benier and Barras, 2006). A simple linear relationship between wetland area and storm surge does not exist, as surge magnitude is affected by factors including the storm's size, wind speeds, track and the shape of the continental shelf (Chen *et al*., 2008). However, wetland loss has allowed storms surges to propagate further inland, increasing the city's vulnerable to storms over time.

The second lesson from Katrina is simply that the climate system is capable of delivering vast quantities of energy. The maximum wind speed of Hurricane Katrina exceeded 77 m s^{-1} (> 175 mph), the maximum eye wall radius reached 110 km and tropical storm force winds extended 370 km from the storm's center (McTaggart-Cowan *et al*., 2007). Storm surges that reached 10.4 m in Biloxi, MS, and ranged between 5.6 – 6.9 m at Shell Beach east of New Orleans, and 3.95 – 4.75 m along the shore of Lake Pontchartrain at the northern edge of the city (Fritz *et al*., 2008). Despite the vast power of Hurricane Katrina, it is important to recognize that the storm did not make landfall at New Orleans. This occurred at Buras, LA and again near Gulfport MS, which are 83 and 68 km from New Orleans, which was on the west, less intense side of the storm (Seed *et al*., 2008).

These two lessons lead to a third, that climate disasters are often the product of an interaction between natural processes and human actions. A smaller storm would have produced a smaller storm surge and less pressure on the levees while properly constructed and maintained levees should have been able to withstand many of Katrina's surges in New Orleans. The catastrophe in New Orleans was exacerbated by inadequate local and federal governmental actions that include a poor assessment of the risks of flooding, an inadequate communication of these risks, poor levee design, poor levee maintenance, and an inadequate ability to evacuate people and provide for them in times of need (Seed *et al*., 2008).

Looking to the future, New Orleans faces threats and opportunities. Global sea levels are predicted to rise, storms may increase in severity and frequency, lands surrounding New Orleans will continue to subside and wetland loss is likely remain problematic. While coastal restoration is needed on a massive scale, New Orleans finds itself hampered by jurisdictional difficulties: many coastal restoration decisions are made by a range of state, federal and local authorities that sometimes must balance restoration against other economic or environmental concerns (Carbonell and Meffert, 2009). While it may be impossible to restore the entire Mississippi Delta plain, sediment loads are high enough to substantially contribute to coastal restoration if managed wisely. Coastal progradation and wetland accretion will likely buffer storm surge and provide opportunities for carbon sequestration. Regional groups are also promoting a "multiple lines of defense" strategy (Lopez, 2006) that views flood protection as an integrated system of natural and man-made components, including barrier islands and beach ridges, wetlands, levees and evacuation plans. New Orleans was settled on high, stable grounds at the mouth of the continent's largest river and this strategic location made it desirable for nations looking to establish a claim to the continent's interior. Such strategic thinking relating a city to its broader environmental assets and liabilities is key to the future of this and perhaps other coastal cities.

Oscillation (AMO), have documented relationships with tropical cyclone activity. For example, when the AMO, a mode of natural variability of sea surface temperatures in the North Atlantic Ocean is in the cold phase, hurricane activity increases (Goldenberg *et al.*, 2001).

As far as changes in hurricane strength and frequency due to anthropogenic climate change go, there is no concrete evidence that global warming is having an influence. Although some scientific studies suggest that warming caused by increased greenhouse gases will increase hurricane intensity (Emanuel, 2005), the connection between the two is not conclusive. There are a number of issues that play into this debate. Sea surface temperatures and upper ocean heat content are very likely to increase in the North Atlantic's main hurricane development regions, and this increase alone will likely favor more intense hurricanes (Emanuel, 2005). However, changes in other key factors (not all of which are mutually exclusive) that influence hurricane number and intensity are more uncertain. These factors include: (1) vertical wind shear, which is dependent on uncertain changes in a range of factors (Vecchi and Soden, 2007) including the ENSO cycle (Gray, 1984; Mann *et al.*, 2009); (2) vertical temperature gradients in the atmosphere (Emanuel, 2007); (3) Saharan dust (Dunion and Velden, 2004; Evan *et al.*, 2006); (4) easterly waves and the West African monsoon (Gray, 1979; Donnelly and Woodruff, 2007); and (5) steering currents, which are influenced by a range of factors including highly uncertain changes in the NAO (Mann *et al.*, 2009).

3.6 Conclusions and key research questions

Climate change is expected to bring warmer temperatures to virtually the entire globe, including all 12 cities analyzed here. Heat events are projected to increase in frequency, severity and duration. Total annual precipitation is expected to increase in

some cities, especially in the mid/high latitudes and tropics, and decrease in other cities, especially in the subtropics. Most cities are expected to experience an increase in the percentage of their precipitation in the form of intense rainfall events. In many cities, droughts are expected to become more frequent, more severe, and of longer duration. Additionally, rising sea levels are extremely likely in all the coastal cities, and are likely to lead to more frequent and damaging flooding related to coastal storm events in the future.

Climate change impacts on cities are enhanced by factors including high population density, extensive infrastructure, and degraded natural environments. Vulnerabilities will be great in many regions that currently experience frequent climate hazards, such as low-lying areas already exposed to frequent flooding. Vulnerabilities will also be large among resource-poor populations, especially in developing countries, where infrastructure may be sub-standard or non-existent, governmental response to disasters may be limited, and adaptation options may be few for reasons including limited capital.

One implication from this chapter is the need for more and improved climate data, especially in cities of developing countries. In many cities, the historical record is either too short or the quality too uncertain to support trend analysis and climate change attribution. Without long historical records, the role of climate variability cannot be adequately described, and climate change projections will not have as strong a historical footing. However, even in cities that have a high quality, lengthy record of temperature and precipitation, there is a need for additional

[ADAPTATION] Box 3.6 Mexico City's Virtual Center on Climate Change

Cecilia Conde, Benjamin Martinez and Francisco Estrada

Centro de Ciencias de la Atmosfera, UNAM

Mexico City's Virtual Center on Climate Change (CVCCCM: www.cycccm-atmosfera.unam.mx/cvcccm/) was created in 2008, with the objectives of: (1) building an entity that concentrates and organizes the information regarding climate change effects on Mexico City, as well as coordinating research efforts on the subject; (2) supporting the continuous development of public policies that aim to increase adaptative capacity and reduce vulnerability of different social sectors; (3) creating an Adaptation, Vulnerability and Mitigation Policy Framework for Mexico City.

The Center aspires to support the development of "useful" science that must answer the questions concerning climate variability and change posed by policymakers of the city.

City authorities have had to deal with extreme events related to the urban heat island, such as heat waves, heavy rains and the resulting floods, and reduced water availability associated with severe droughts in the catchment basin from which the city satisfies part of its water demand.

Generally, it could be said that cities now experience what could occur under projected climate change scenarios. For example, systems outside of Mexico City might be resilient to an increase of 1 °C in mean temperatures, but in the city the warming process has already reached more than 3 °C (Jauregui, 1997).

As a consequence of the uncontrolled growth of the city's population and urbanization area, the increase in the occurrence of heavy rains since the 1960s has led to an increase in the frequency of severe floods. This provides an example of Mexico City's high sensitivity to climate change.

The Virtual Center must be seen as necessary to face the climatic problems that could increase in the future.

The research priorities selected by the City Government are:

1. Assessment of Mexico City air quality, the effect on the health of people exposed to allergenic bio-particles (pollen), and its relation to climate change
2. Effect of the interaction of temperature and ozone on Mexico City's hospital admissions
3. The impact of climate change on water availability in the Metropolitan Area of Mexico City
4. Vulnerability of potable water sources in Mexico City in the context of climate change
5. Energy consumption scenarios and emission of greenhouse gases produced by the transport sector in the Metropolitan Area of Mexico City
6. Assessment of the impacts in the Metropolitan Area of Mexico City related to solid waste under climate change conditions
7. Vulnerability of the ground of conservation of Mexico City to climate change and possible adaptation measures
8. Determination of the vulnerability of the conservation areas of Mexico City to climate change and possible adaptation measures

Of course, several problems have been detected during the development of this Virtual Center. In particular, "traditional" science has not yet been capable of achieving interdisciplinary research and being stakeholder driven. Currently, researchers are devoted to publishing papers instead of "translating" information for decision-making. Most of the policymakers' decisions are more focused on resolving the immediate problems than on designing long-term strategies.

The actors of this Virtual Center are aware of these barriers, and these problems are being confronted, for example, through periodic meetings with diverse authorities of Mexico City, which allow direct answers to their questions. This motivates a rich discussion from different points of view, resulting in joint strategies that facilitate the incorporation of the found solutions into public policies. It is expected that this critical stage of the research could be fulfilled during 2010, when partial results will be presented to Mexico City's authorities.

station data and climate variables at high temporal resolution to improve our understanding of the microclimates that help define the urban setting and climate risk. If these data can be integrated into monitoring systems and real time networks – which can be an expensive proposition for some cities – weather forecasting can be improved as well.

Furthermore, improved monitoring can help bridge the gaps between weather and climate, and climate regions and cities. This active area of research will enable analysts to use real-time ocean temperatures to better discern how the frequency of extreme events (including hurricanes) may vary by decade in the future. As predictions improve, adaptation strategies can be tailored to reflect these advances. Monitoring must include impact variables identified by stakeholders, such as water reservoir levels, frequency of power failures, and transportation delays. It is critical that this information not only be collected but also stored systematically in a unified database that facilitates the sharing of information and research results across agencies and cities.

Given the range of climate hazards and impacts described here, there is a critical need for climate change adaptation strategies that align with societal goals such as development, environmental protection (including greenhouse gas mitigation), and social justice and equity.

REFERENCES

Arrhenius, S. (1896). On the influence of carbonic acid in the air upon the temperature of the ground. *London, Edinburgh, and Dublin Philosophical Magazine and Journal of Science* (fifth series), **41**, 237–275.

Australian Bureau of Meteorology (2009). Climate information. www.bom.gov.au/climate/.

Balling, R. C. and S. W. Brazel (1987). Diurnal variations in Arizona monsoon precipitation. *Monthly Weather Review*, **115**, 342–346.

Barras, J. *et al*. (2003). *Historical and Projected Coastal Louisiana Land Changes*: 1978–2050. USGS.

Bornstein, R. and M. LeRoy (1990). Urban barrier effects on convective and frontal thunderstorms. *Fourth Conference on Mesoscale Processes*, American Meteorological Society, 2.

Burian, S. J. and J. M. Shepherd (2005). Effect of urbanization on the diurnal rainfall pattern in Houston. *Hydrological Processes*, **19**, 1089–1103.

Carbonell, A. and Meffert, D. J. (2009). *Climate Change and the Resilience of New Orleans: the Adaptation of Deltaic Urban Form*. Commissioned Research Report for the World Bank 2009 Urban Research Symposium, Marseilles, France.

Census of Canada (2006). Statistics Canada, accessed 2010, www.statcan.gc.ca/.

Changnon, S. A. (1968). The La Port weather anomaly – fact or fiction? *Bulletin of the American Meteorological Society*, **49**, 4–11.

Changnon, S. A. and N. E. Westcott (2002). Heavy rainstorms in Chicago: Increasing frequency altered impacts, and future implications. *Journal of American Water Resources*, **48**, 1467–1475.

Charlson, R. J., S. E. Schwartz, J. M. Hales, *et al.* (1992). Climate forcing by anthropogenic aerosols. *Science*, **255**, 423–430.

Chen, T. C., S. Y. Wang, and M. C. Yen (2007). Enhancement of afternoon thunderstorm activity by urbanization in a valley: Tapei. *Journal of Applied Meteorology and Climatology*, **46**, 1324–1340.

Chen, Q., Wang, L. and Tawes, R. (2008). Hydrodynamic response of northeastern Gulf of Mexico to Hurricanes. *Estuaries and Coasts* **31**, 1098–1116.

Christensen, J.H., *et al*. (2007) Regional Climate Projection. *Climate Change 2007: The Physical Science Basis. Contribution of Working Group I to the Fourth Assessment Report of the Intergovernmental Panel on Climate Change*, eds. S. Solomon, *et al*. Cambridge University Press, 849–940.

Coleman, J. M., Roberts, H. H. and Stone, G. W. (1998). The Mississippi Delta: An overview. *Journal of Coastal Research* **14**, 698–716.

Coleman, J. M. and Prior, D. B. (1980). Deltaic Sand Bodies. 171.

Collins, M. (2005). El Nino- or La Nina-like climate change? *Climate Dynamics*, **24**, 89–104.

Cunha, L. R. and M. Miller Santos (1993). The Rio reconstruction project: the first two years. In *Towards A Sustainable Urban Environment: The Rio de Janeiro Study*, World Bank Discussion Paper 195, Washington, DC, USA: World Bank.

Day, J. W. *et al*. (2007). Restoration of the Mississippi Delta: Lessons from Hurricanes Katrina and Rita. *Science*, **315**, 1679–1684.

Dixon, T. H. *et al*. (2006). Subsidence and flooding in New Orleans. *Nature* **441**, 587–588.

Dilley, M. (2000). Reducing vulnerability to climate variability in Southern Africa: the growing role of climate information. *Climatic Change*, **45**, 63–73.

Donnelly, J. P. and J. D. Woodruff (2007). Intense hurricane activity over the past 5,000 years controlled by El Nino and the West African monsoon. *Nature*, **447**, 465–468.

Dunion, J. P. and C. S. Velden (2004). The impact of the Saharan air layer on Atlantic tropical cyclone activity. *Bulletin of the American Meteorological Society*, **85**, 353–365.

Emanuel, K. (2005). Increasing destructiveness of tropical cyclones over the past 30 years. *Nature*, **436**, 686–688.

Emanuel, K. (2007). Environmental factors affecting tropical cyclone power dissipation. *Journal of Climate*, **20**, 5497–5509.

Emanuel, K. (2008). Hurricanes and global warming: results from downscaling IPCC AR4 simulations. *Bulletin of the American Meteorological Society*, **89**, 347–367.

Environment Canada (2009). Canada's National Climate and Weather Data Archive. www.climate.weatheroffice.gc.ca.

Eri, S., N. Aishali, and L. W. Horowitz (2009). Present and potential future contributions of sulfate, black and organic carbon aerosols from China to global air quality, premature mortality and radiative. *Atmospheric Environment*, **43**, 2814–2822.

Evan, A. T., J. P. Dunion, J. A. Foley, A. K. Heidinger, and C. S. Velden (2006). New evidence for a relationship between Atlantic tropical cyclone activity and African dust outbreaks. *Geophysical Research Letters*, **33**, L19813, doi:19810.11029/12006GL026408.

Fairbanks, R. G. (1989). 17,000-year glacio-eustatic sea level record: influence of glacial melting rates on the Younger Dryas event and deep-ocean circulation. *Nature*, **342**, 637–642.

Fernandes, E. (2000). The legalisation of favelas in Brazil: problems and prospects. *Third World Planning Review*, **22**(2), 167–188.

Fritz, H. M. *et al.* (2008). Hurricane Katrina storm surge reconnaissance. *Journal of Geotechnical and Geoenvironmental Engineering* **134**, 644–656.

Gaffin, S. R., C. Rosenzweig, R. Khanbilvardi, *et al.* (2008). Variations in New York City's urban heat island strength over time and space. *Theoretical and Applied Climatology*, **94**, 1–11.

Gao, X., L. Yong, and W. Lin (2003). Simulation of effects of land use change by a regional climate model. *Advances in Atmospheric Sciences*, **20**, 583–592.

Goldenberg, S. B., C. Landsea, A. M. Mestas-Nunez, and W. M. Gray (2001). The recent increase in Atlantic hurricane activity: causes and implications. *Science*, **293**, 474–479.

Gould, H. R. (1970), in *Deltaic Sedimentation* Vol. Special Publication 15, ed. J. P. Morgan. Society of Economic Paleontologists and Mineralogists.

Gray, W. M. (1979). Hurricanes: their formation, structure, and likely role in the tropical circulation. In D. B. Shaw (Ed.), *Meteorology Over the Tropical Oceans*, London, UK: Royal Meteorological Society, pp. 155–218.

Gray, W. M. (1984). Atlantic seasonal hurricane frequency. Part I: El Nino and 30 mb quasi-biennial oscillation influences. *Monthly Weather Review*, **112**, 1649–1668.

Grimm, A. M. (2000). Climate variability in southern South America associated with El Nino and La Nina events. *Journal of Climate*, **13**, 35–58.

Grimm, A. M. (2003). The El Nino impact on the summer monsoon in Brazil: regional processes versus remote influences. *Journal of Climate*, **16**, 263–280.

Grimm, A. (2004). How do La Niña events disturb the summer monsoon system in Brazil? *Climate Dynamics*, **22**, 123–138

Grimm, A. M. and R. G. Tedeschi (2009). ENSO and extreme rainfall events in South America. *Journal of Climate*, **22**, 1589–1609.

Gupta, P., S. A. Christopher, J. Wang, *et al.* (2006). Satellite remote sensing of particulate matter and air quality assessment over global cities. *Atmospheric Environment*, **40**, 5880–5892.

Gusmão, P. P., P. Serrano do Carmo, and S. B. Vianna (2008). *Rio Proximos 100 Anos*. Rio De Janiero, Brazil: Instituto Municipal de Urbanismo Pereira Passos.

Guttman, N. B. (1989). Statistical descriptors of climate. *Bulletin of the American Meteorological Society*, **70**, 602–607.

Hachadoorian, L., S. R. Gaffin, and R. Engelman (2011). Mapping the population future: projecting a gridded population of the World using ratio methods of trend extrapolation. In R. P. Cincotta and L. J. Gorenflo (Eds.), *Human Population: The Geography of* Homo Sapiens *and its Influence on Biological Diversity*, Heidelberg,Germany: Springer-Verlag.

Harshvardhan, S., E. Schwartz, C. M. Benkovitz, and G. Guo (2002). Aerosol influence on cloud microphysics examined by satellite measurements and chemical transport modeling. *Journal of the Atmospheric Sciences*, **59**, 714–725.

Hoerling, M. P., A. Kumar, and M. Zhong (1997). El Nino, La Nina and the nonlinearity of their teleconnections. *Journal of Climate*, **10**, 1769–1786.

Horton, R. E. (1921). Thunderstorm breeding spots. *Monthly Weather Review*, **49**, 193.

Horton, R. (2007). *An Observational and Modeling Study of the Regional Impacts of Climate Variability*, Columbia University.

Horton, R., C. Herweijer, C. Rosenzweig, *et al.* (2008). Sea level rise projects for the current generations CGCMs based on the semi-empirical method. *Geophysical Research Letters*, **35**.

Horton, R., V. Gornitz, M. Bowman, and R. Blake (2010). *Climate observations and projections*. Ann. New York Acad. Sci., 1196, 41–62, doi:10.1111/j.1749–6632.2009.05314.x.

Horton, R., and C. Rosenzweig (2010). *Climate Risk Information*. Ann. New York Acad. Sci., 1196, 147–228, doi:10.1111/j.1749–6632.2010.05323.x.

Howard, L (1820). *The Climate of London, Deduced from Meteorological Observations, Made at Different Places in the Neighbourhood of the Metropolis. 2*, London, 1818–1820.

Huff, F. A. and S. A. Changnon (1972a). Climatological assessment of urban effects on precipitation at St. Louis. *Journal of Applied Meteorology*, **11**, 823–842.

Huff, F. A. and S. A. Changnon (1972b) *Climatological Assessment of Urban Effects on Precipitation St. Louis: Part II. Final Report*, NSF Grant GA-18781, Illinois State Water Survey.

Hurrell, J. W. (1995). Decadal trends in the North Atlantic Oscillation and relationships to regional temperature and precipitation. *Science*, **269**, 676–679.

Hurrel, J. W., Y. Kushnir, G. Ottersen, and M. Visbeck (2003). An overview of the North Atlantic Oscillation. In J. W. Hurrell *et al.* (Eds.), *The North Atlantic Oscillation: Climatic Significance and Environmental Impact*, Geophysical Monograph 134, Washington, DC, USA: American Geophysical Union, pp. 1–35.

Ichinose, T. and Y. Bai (2000). Anthropogenic heat emission in Shanghai City. In *Proceedings of Annual Meeting of Environmental Systems Research*, Vol. 28, pp. 329–337.

IPCC (2007). *Climate Change 2007: The Physical Science Basis. Contribution of Working Group I to the Fourth Assessment Report of the Intergovernmental Panel on Climate Change*, Cambridge, UK: Cambridge University Press.

Jáuregui, E. (1997). Heat island development in Mexico City. *Atmospheric Environment*, **31**(22), 3821–3831.

Jauregui, E. and E. Romales (1996). Urban effects on convective precipitation in Mexico City. *Atmospheric Environment*, **30**, 3383–3389.

Jiong, S. (2004). Shanghai's land use pattern, temperature, relative humidity and precipitation. *Atlas of Shanghai Urban Physical Geography*.

Karl, T. R. and R. W. Knight (1998). Secular trends of precipitation amount, frequency and intensity in the United States. *Bulletin of the American Meteorological Society*, **79**, 231–241.

Kaufmann, R. K., K. C. Seto, A. Schneider, *et al.* (2007). Climate response to rapid urban growth: evidence of a human-induced precipitation deficit. *Journal of Climate*, **20**, 2299–2306.

Kolb, C. R. and Saucier, R. T. (1982). Engineering geology of New Orleans. *Review of Engineering Geology* **5**, 75–93.

Kothawale, D. R. and K. Rupa Kumar (2005). On the recent changes in surface temperature trends over India. *Geophysical Research Letters*, **32**.

Kratzer, P. (1937). *Das stadtklima*, Braunschweig: F.Viewg uE Sohne.

Kratzer, P. (1956). *Das stadtklima* (2nd edition), Braunschweig: F Vieweg uE Sohn (tranlated by the U.S. Air Force, Cambridge Research Laboratories).

Landsberg, H. (1956). The climate of towns. In W. L. Thomas (Ed.), *Man's Role in Changing the Face of the Earth*, Chicago, IL, USA: The University of Chicago Press.

Landsberg, H. E. (1970). Man-made climate changes. *Science*, **170**, 1265–1274

Lawrence, M. B. and J. M. Gross (1989). Annual summaries: Atlantic hurricane season of 1988. *Monthly Weather Review*, **117**, 2248–2459.

Lian, L. and J. Shu (2007). Numerical simulation of summer climate over center and east China using a regional climate model. *Journal of Tropical Meteorology*, **23**, 162–169.

Liu, K. B. and Fearn, M. L. (2000). Reconstruction of prehistoric landfall frequencies of catastrophic hurricanes in northwestern Florida from lake sediment records. *Quaternary Research* **54**, 238–245.

Lopez, J. A. (2007). *The Multiple Lines of Defense Strategy to Sustain Coastal Louisiana*. Lake Pontchartrain Basin Foundation, New Orleans.

Mann, M. E., J. D. Woodruff, J. P. Donnelly, and Z. Zhang (2009). Atlantic hurricanes and climate over the past 1,500 years. *Nature*, **460**, 880–883.

Marengo, J. A. and C. C. Camargo (2008). Surface air temperature trends in Southern Brazil for 1960–2002. *International Journal of Climatology*, **28**, 893–904.

McTaggart-Cowan, R., Bosart, L. F., Gyakum, J. R. and Altallah, E. H. (2007). Hurricane Katrina (2005) Part 1: Complex life cycle of an intense tropical cyclone. *Monthly Weather Review* **135**, 3905–3926.

Morton, R. A., Benier, J. C. and Barras, J. A. (2006). Evidence of regional subsidence and associated interior wetland loss induced by hydrocarbon production, Gulf Coast region, USA. *Environmental Geology* **50**, 261–274.

Nakicenovic, N. and Coauthors (2000). *Special Report on Emissions Scenarios: A Special Report of Working Group III of the Intergovernmental Panel on Climate Change*, Cambridge, UK: Cambridge University Press.

Nastos, P. T. and C. S. Zerefos (2007). On extreme daily precipitation totals at Athens, Greece. *Advances in Geosciences*, **10**, 59–66.

National Climatic Data Center, Global Historical Climatology Network: Version 2 (2008). www.ncdc.noaa.gov/oa/climate/ghcn-monthly/index.php.

Nelson, S. A. and LeClair, S. F. (2006). Katrina's unique splay deposits in a New Orleans neighborhood. *GSA Today* **16**, 4–10, doi: 10.1130/GSAT01609A.1.

Ohashi, Y., Y. Genchi, H. Kondo, *et al.* (2007). Influence of air-conditioning waste heat on air temperature in Tokyo during summer: numerical experiments using an urban canopy model coupled with a building energy model. *Journal of Applied Meteorology and Climatology*, **46**, 66–81.

Oke, T. R. (1987). *Boundary Layer Climates* (2nd edition), London, UK: Routledge.

Orr, J. C., Fabry, V. J., Aumont, O., *et al.* (2005). Anthropogenic ocean acidification over the twenty-first century and its impact on calcifying organisms. *Nature*, **437**, 681–686.

Parson, E., V. Burkett, K. Fisher-Vanden, *et al.* (2007). Global change scenarios: their development and use. Sub-report 2.1B of *Synthesis and Assessment Product 2.1 by the US Climate Change Science Program and the Subcommittee on Global Change Research*, Washington, DC, USA: Department of Energy, Office of Biological and Environmental Research, p. 106.

Pawan, G., C. A. Sundar, and W. Jun (2006). Satellite remote sensing of particulate matter and air quality assessment over global cities. *Atmospheric Environment*, **40**, 5880–5892.

Pielke, R. A. (2005). Land use and climate change. *Science*, **310**, 1625–1626.

Reed, D. J. (2002). Sea-level rise and coastal marsh sustainability: geological and ecological factors in the Mississippi delta plain. *Geomorphology* **48**, 233–243.

Ren, G. Y., Z. Y. Chu, Z. H. Chen, and Y. Y. Ren (2007). Implications of temporal change in urban heat island intensity observed at Beijing and Wuhan stations, *Geophysical Research Letters*, **34**, L05711, doi:10.1029/2006GL027927.

Rignot, E. and P. Kanagaratnam (2006). Changes in the velocity structure of the Greenland ice sheet. *Science*, **311**, 986–990.

Rogers, J. D. *et al*. (2008). Geological Conditions Underlying the 2005 17th Street Canal Levee Failure in New Orleans. *Journal of Geotechnical and Geoenvironmental Engineers* **134**, 583–601.

Ropelewski, C. (1999). The Great El Nino of 1997 and 1998: impacts on precipitation and temperature. *Consequences*, **5**, 17–25.

Rosenzweig, C., W. D. Solecki, L. Parshall, and S. Hodges (Eds.) (2006). *Mitigating New York City's Heat Island with Urban Forestry, Living Roofs, and Light Surfaces*, New York City Regional Heat Island Initiative, Final Report 06–06, New York State Energy Research and Development Authority.

Russel, G. (2005) in *The Times Picayune* Vol. 169 A1 (New Orleans, 2005).

Sanderson, E. and M. Boyer (2009). *Mannahatta: A Natural History of New York City*, New York, USA: Abrams Books.

Satterthwaite, D. (2008). Cities' contribution to global warming: notes on the allocation of greenhouse gas emissions. *Journal of Environment and Urbanization*, **20**, 539–549.

Seed, R. B. *et al*. (2008). New Orleans and Hurricane Katrina 1: Introduction, overview, and the east flank. *Journal of Geotechnical and Geoenvironmental Engineering* **135**, 701–739.

Selover, N. (1997). Precipitation patterns around an urban desert environment: topographic or urban influences? *Association of American Geographers Convention*, **2**.

Shepherd, J. M. (2005). A review of current investigations of urban-induced rainfall and recommendations for the future. *Earth Interactions*, **9**, 1–27.

Shepherd, J. M. (2006). Evidence of urban-induced precipitation variability in arid cliamte regimes. *Journal of Arid Environments*, **67**, 607–628.

Shepherd, J. M., H. Pierce, and A. J. Negri (2002). Rainfall modification by major urban areas: observations from spaceborne rain radar on the TRMM satellite. *Journal of Applied Meteorology*, **41**, 689–701.

Shu, J., J. A. Dearing, A. P. Morse, L. Yu, and C. Li (2000). Magnetic properties of daily sampled total suspended particulates in Shanghai. *Environment Science and Technology*, **34**, 2393–2400.

Shu, J., J. A. Dearing, A. P. Morse, L. Yu, and N. Yuan (2001). Determining the sources of atmospheric particles in Shanghai, China, from magnetic and geochemical properties. *Atmospheric Environment*, **35**, 2615–2625.

Simpson, M. D. (2006). *Role of Urban Land Use on Mesoscale Circulations and Precipitation*, North Carolina State University.

Stout, G. E. (1962). Some observations of cloud initiation in industrial areas. In *Air Over Cities*, Technical Report A62–5. Washington, DC: US Public Health Service. Tayanc, M. and H. Toros (1997). Urbanization effects on regional climate change in the case of four large cities of Turkey. *Climate Change*, **35**, 501–524.

Tornqvist, T. E. *et al*. (2008). Mississippi Delta subsidence primarily caused by compaction of Holocene strata. *Nature Geoscience* **1**, 173–176.

Trenberth, K. (1984). Signal versus noise in the Southern Oscillation. *Monthly Weather Review* **112**, 326–332

Trenberth, K. E. and J. M. Caron (2000). The Southern Oscillation revisited: sea level pressures, surface temperatures and precipitation. *Journal of Climate*, **13**, 4358–4365.

Trenberth, K. E. and Fasullo, J. (2008). Energy budgets of Atlantic hurricanes and changes from 1970. *Geochemistry, Geophysics, Geosystems* **9**, doi:2007GC001847.

UK Met Office and Hadley Centre (2009). Observations datasets. http://hadobs.org/.

UNFPA (2007). *The State of World Population 2007*. United Nations Population Fund, United Nations Publications.

UN-HABITAT (2006). *State of the World's Cities*, London, UK: Earthscan.

United Nations Statistical Division Demographic Yearbook (2010). http://unstats.un.org/unsd/demographic/products/dyb/dyb2007.htm.

Vecchi, G. A. and B. J. Soden (2007). Increased tropical Atlantic wind shear in model projections of global warming. *Geophysical Research Letters*, **34**, L08702, doi:08710.01029/02006GL028905.

Velicogna, I. and J. Wahr (2006). Acceleration of Greenland ice mass loss in spring 2004. *Nature*, **443**, 329–331.

Visbeck, M. H., J. W. Hurrell, L. Polvani, and H. M. Cullen (2001). The North Atlantic Oscillation: past, present, and future. *Proceedings of the National Academy of Sciences*, **98**, 12,876–12,877.

Wilby, R. L., G. O'Hare, and N. Barnsley (1997). The North Atlantic Oscillation and British Isles climate variability. *Weather*, **52**, 266–276.

Yin, J., M. E. Schlesinger, and R. J. Stouffer (2009). Model projections of rapid sea-level rise on the northeast coast of the United States. *Nature Geoscience*, **2**, 262–266.

Zhang, X., L. A. Vincent, W. D. Hogg, and A. Niitsoo (2000). Temperature and precipitation trends in Canada during the 20th century. *Atmosphere-Ocean*, **38**, 395–429.

Zheng Yiqun, Qian Yongfu, Miao Manqian, *et al.* (2002). The effects of vegetation change on regional climate I: Simulation results. *Acta Meteorologica Sinica*, **60**, 1–16 (in Chinese).